Distance Protection Challenges in a Wind Farm

Kasper de Korte

Master Thesis

Distance Protection Challenges in a Wind Farm

by

Kasper de Korte

to obtain the degree of Master of Science
at the Delft University of Technology,
to be defended publicly on Wendsday March 13, 2019 at 13:00 AM.

Student Number:	4372700
Report Type:	Master thesis
Master Program:	Electrical Engineering
Master Track:	Electrical Power Engineering
Company:	Siemens Nederland N.V.
Company Address:	Pr. Beatrixlaan 800, 2595BN Den Haag
Project duration:	June 1, 2018 – March 13, 2019

Thesis committee:

Dr.ir. M. Popov,	TU Delft	+31 (0)15 2786219
Prof.ir. M.A.M.M. van der Meijden,	TU Delft	+31 (0)15 2788907
Dr.ir. Z. Qin,	TU Delft	+31 (0)15 2786584
Ir. G. M. Van Dijk,	Siemens Nederland N.V.	+31 (0) 6 19281922
Dr.ir. J.J. Chavez Muro,	TU Delft	+31 (0)15 2786239

This thesis is confidential and cannot be made public until March 13, 2020.

TU Delft

SIEMENS
Ingenuity for life

Abstract

Wind farms are currently built in the North Sea in the Netherlands. The grid connecting the off-shore wind farm to the main-land distribution grid must be protected against short-circuits and other electrical disturbances.

In this project is studied if electrical protection of a grid is suitable for grids connecting renewable energy sources to the transmission grid. The research question is as follows: Does the distance protection function of a protection relay respond correctly to all faults in a wind farm electrical grid?

The research question is tried to be answered through simulations and tests. Faults are simulated, and a part of the grid is tested in a real protection relay. The results of these tests show that the protection relay does not always react as expected. Results are analyzed to explain these unexpected results. A situation with a three-phase fault and a situation with a two-phase to ground fault caught the attention. These two unexpected results are analyzed with calculations to explain the behavior and find the cause. The calculations give more insight, but no single solution has been found. Recommendations are given to reduce the change of undesired behavior of the protection relay.

Contents

Abstract I

List of Abbreviations IV

1 Introduction 1
- 1.1 Project Description . . . 1
- 1.2 Scientific Contribution . . . 2
- 1.3 Research Questions . . . 2
  - 1.3.1 Hypothesis . . . 3
- 1.4 Scope . . . 3
- 1.5 Technical Process . . . 3
  - 1.5.1 Simulation Model . . . 3
  - 1.5.2 Scenarios . . . 3
  - 1.5.3 Signal Extraction and Synthesis . . . 3
  - 1.5.4 Test . . . 4
  - 1.5.5 Analysis . . . 4
  - 1.5.6 Discussion and Conclusion . . . 4

2 Protection Relay Setup 5
- 2.1 Protection Against Faults . . . 5
  - 2.1.1 Current and Voltage Measurement . . . 5
- 2.2 Fault Detection . . . 6
  - 2.2.1 Distance Protection . . . 6
  - 2.2.2 Power Direction Determination . . . 7
  - 2.2.3 Zone Setting . . . 7
  - 2.2.4 Impedance Calculation . . . 8
  - 2.2.5 Signal Processing . . . 9
  - 2.2.6 Filtering . . . 9
- 2.3 Challenges in Protection . . . 9

3 Description of the study case network 11
- 3.1 General Overview of the Grid . . . 11
- 3.2 Faults . . . 15
  - 3.2.1 Fault Resistance . . . 15
- 3.3 Testing and Modeling Methods . . . 16
  - 3.3.1 Analytical Model . . . 16
  - 3.3.2 Full Simulation . . . 16
  - 3.3.3 Partly simulation with Real Equipment Testing . . . 17

3.4 Grid Model . . . 17
3.4.1 Wind Turbine Model . . . 17
3.4.2 Transformers and reactors . . . 19
3.4.3 Cables . . . 20
3.5 Distance Protection Settings . . . 24

4 Simulation and Test 25
4.1 Data Management . . . 26
4.1.1 Power Dependent Grid Settings . . . 26
4.1.2 Comtrade File Format . . . 27
4.2 Simulation Automation . . . 27
4.2.1 Script . . . 27
4.2.2 Output of the Simulation . . . 28
4.3 Test . . . 29
4.3.1 Protection Relay Settings . . . 29
4.3.2 Test Setup . . . 29
4.3.3 Procedure . . . 31

5 Analysis 32
5.1 Protection Relay Response . . . 32
5.1.1 Analysis Tool . . . 32
5.2 Results . . . 33
5.2.1 Unexpected results with a clear cause . . . 35
5.3 Unexpected Results Explained in Detail . . . 37
5.3.1 Unexpected result 5: Changing Impedance and Voltage Angle . . . 37
5.3.2 Unexpected result 6: Arc-resistance reduces calculated impedance . 41
5.4 Remarks on shunt reactor . . . 46

6 Discussion 47
6.1 Challenges in protection . . . 47
6.2 Grid . . . 48
6.3 Unexpected results . . . 49
6.4 Developed tools . . . 50
6.4.1 Database . . . 50
6.5 Improvements and Further research . . . 50
6.5.1 grid model expansion . . . 50
6.5.2 Increase automation . . . 51
6.6 Advice for future protection schemes . . . 51

7 Conclusion 53

Appendices 57
Appendix 1: Scenario List . . . 58
Appendix 2: Positive Sequence Circuit Decompositon for Unexpected Result 5 . . 62
Appendix 3: Sequential sequence Circuit decompositon for Unexpected Result 6 68
Appendix 4: Determination of the real loop impedance of unexpected result 6 . 75

List of Abbreviations

AC alternating current. 17

CB circuit breaker. 5, 15, 30, 47
CMC calibrator for measurement converters. VI, 3, 26, 30, 31, 51
CT current transformer. 5, 7, 13, 14, 20, 29, 53

DC direct current. 17
DFIG doubly fed induction generator. 14, 17, 18
DG distributed generation. 1

EMT electromagnetic transient. 3, 17, 18, 25, 43

FIR finite impulse response. 9

IT instrument transformer. VI, 5, 6, 13, 20, 25, 52

L-G line to ground. V, 3, 8, 19, 24, 26, 35, 36, 41, 43, 47, 50, 52

MPT maximum power tracker. 19

PEC power electronic converter. 1, 9, 17, 18, 19
PI-controller proportional-integral controller. 19

RCF residual compensation factor. 8, 10, 36, 37, 45, 46, 48, 51, 52, 53
RES Renewable energy source. 1, 3, 10
RMD distance protection with the reactance method. 6, 9, 41, 46, 52

SCR short circuit ratio. 17
SLD single line diagram. 11

Trf 1 transformer 1. 36, 48, 51
Trf 2 transformer 2. 14

VT voltage transformer. 5, 13, 20, 53

WPP wind power plant. 1, 14, 45
WT wind turbine. 3, 10, 14, 17, 18, 19, 26, 35, 37, 41, 48, 49, 50, 51, 53
WTG wind turbine generator. 18

List of Figures

2.1 Three phase setup of the protection relay. 6
2.2 The relation between the zone-parameters and the quadrilateral shape. . . 7

3.1 Simplified overview of the wind farm grid as modeled including fault locations. 12
3.2 Single line diagram symbol of a current transformer 3.2a and voltage transformer 3.2b. 13
3.3 Configurations of modeling a fault resistance for a L-L fault (3.3a) a L-L-G fault (3.3b) and a L-L-L fault (3.3c). 16
3.4 Schematic diagram of a type 3 (DFIG) wind turbine. 18
3.5 Simplified control loop of the DigSilent WTG model. 18
3.6 A cable can be modeled with an impedance in series and two in parallel. . . 21
3.7 Distributed parameter model using the Bergeron method. 21
3.8 Frequency response (3.8a) and phase resoponce (3.8b) of four cable model configurations. 23
3.9 Example of a unfiltered line to ground (L-G) and L-L reactance over time with a fault initiated at 0.5 s with two cable models. 24

4.1 Test setup; photo (4.1a) and diagram (4.1b). 30

5.1 Simplified overview of the wind farm grid as modeled including fault locations. 34
5.2 Impedance plot of a scenario with an unexpected result. 35
5.3 Impedance plot L-G fault at F4 measured at RD1. 36
5.4 Impedance plot of RD3 (5.4a) and RD2 (5.4b). 38
5.5 Equivalent positive sequence circuit including a thee phase fault at location F2. 39
5.6 Impedance plot of RD3, result for the hand calculation and IEC 60909 and the EMT simulation result where the wind turbine control is tuned off . . . 40
5.7 Simplified representation of the grid with a L-L-G fault at location F1. . . . 42
5.8 Impedance plot the L-G fault loop impedance measured with RD3. 42
5.9 Sequential components network of a L-L-G fault at fault location F1 43
5.10 Plot of the impedance measured by RD3 for different fault impedances . . 44
5.11 Typical fault loop which is used as a basis for the impedance calculation (5.11a) and the real fault loop for this scenario (5.11b). The solid line is the fault loop, the dotted line is part of the system that influence the fault loop. 44

A2-1 Equivalent positive sequence circuit including a thee phase fault at location F2. 62
A2-2 Equivalent positive sequence circuit where the WPP and transformer 2 are merged in normal condition. 65
A2-3 Equivalent positive sequence circuit where the WPP and transformer 2 are merged. 66
A3-1 Equivalent sequential sequence circuit including a thee-phase fault at location F2. 69
A3-2 Impedances in a L-L-G fault in a three phase system 71
A4-1 $L_B - G$ fault loop with influencing circuit in dashed line. 75
A4-2 $L_A - L_B$ fault loop with influencing circuit in dashed line. 78

List of Tables

3.1 Location of the faults in the simulation. 15
3.2 Arc Resistance, minimum short circuit current and arc length for different types of faults at locations F1 and F2. 15
3.3 Ratios of the instrument transformers (ITs). 20
3.4 Distance zone settings for protection relays RD1, RD2 and RD3. 24

4.1 Scenario dependent equipment settings. 25
4.2 Devices and software used in the test setup. 29
4.3 Cable connections between the calibrator for measurement converters (CMC) and the protection relay. 30

5.1 Parameters of the scenario for the unexpected results groups. 33
5.2 Important time points during these scenarios. 38

A2-1 Input parameters to calculate the positive sequence circuit. 63
A3-1 Positive and negative sequence impedances. 69
A3-2 Parameters to calculate the zero sequence impedances. 70
A3-3 Line voltages and currents at fault location and at RD3 73
A4-1 Voltages, currents and impedances in the fault loop that effect the fault loop impedance. 76

Chapter 1

Introduction

The installed capacity of renewable energy sources is increasing faster than other energy sources. The two reports of GWEC and SolarPower europe [1, 2] have been published with both different scenarios of the future energy production. All scenarios predict that the increasing trend of integration of wind and solar energy will continue. Governments steer to more RES to reduce the CO2 emissions and dependencies of fossil fuels [3]. The properties of wind and solar energy are different from synchronous generators with a large inertia. One of these properties is that wind and solar energy are often distributed generations (DGs) instead of the centralized generation. An increase of proportion of wind and solar energy change the behavior of the grid. Fault protection of the grid must adapt to this change. This topic of fault protection in grids with a power electronic converter (PEC) connected DG is already addressed in 1982 [4, 5]. Technology is changed since that time for both protection and PEC. Especially for the distance protection function in combination of DG failures are reported in litrature [6, 7]. Since a couple of years this topic is relevant for the electricity grid in the Netherlands because of the mass integration of renewable energy sources (RESs) especially wind power.

1.1 Project Description

The objective of this project is to identify potential problems with the protection of a grid with high penetration of RES and find its cause. In order to have a realistic case, a protection scheme of the Borsele off-shore wind power plant (WPP) is studied. An offshore grid connects the wind turbines to the on shore transmission grid. The protection scheme of this transmission system uses multiple types of protection methods. In this graduation project only the distance protection of the offshore transmission grid is considered.

A detailed model of the grid is made in power engineering software. Part of the simulation will be extracted and synthesized so that real protection devices can be involved. The behavior of the protection relay is analyzed. Unexpected behavior is studied. The result of the analysis can point out parts of the protection scheme that needs to be improved or conform that it works as desired.

1.2 Scientific Contribution

Based on the results of simulation and tests, unexpected behavior could be detected, and mitigating measures can be proposed. Unexpected behavior could occur in protection relays. Similar studies have been carried out on this topic and earlier studies have shown that there is a difference in vendor of protection devices if it comes to certainty of tripping [1]. New insights in the protection scheme can help further projects to improve the protection scheme. This can eventually result in an optimization of the grid protection and therefore decrease the unavailability of the electricity grid. An improvement in this project can make a minor move in technology. The project is carried out in steps according to the scientific method: Question, hypothesis, prediction, test, analyzing and publication.

This project is unique because a real grid is used. Similar studies are carried out where hypothetical grids are used. Focusing on a grid that will be build can potentially give more useful results.

Although there has been chosen to focus on one grid, it is important to keep the project general. This is to keep the results useful for other cases.

Literature will be consulted for potential problems which may arise on the detection of faults in the grid. The findings from literature steers the project to investigate certain power system equipment or situations.

1.3 Research Questions

One main question is the common thread through this project. Several sub-questions have been asked to support the main question. The main question is:

"Does the conventional distance protection relay respond correctly to all faults in a wind farm electrical grid?"

Sub questions are:

1. What is a good method to test the response of a protection relay on the dynamic behavior of the grid?
2. How does an autotransformer effect the impedance determination in the protection relay?
3. Does the distance protection function of a protection relay handle the dynamic behavior of a wind turbine correctly?
4. What issues can disturb the function of the distance protection function in the protection relay?
5. Can a fault in a shunt reactor be detected with the distance protection function of a protection relay?

1.3.1 Hypothesis

It is expected that the distance protection in the protection relay will respond correctly to the tested scenarios. There is more than 80 years' experience with distance protection [8].

The power electronics controlled RES are a relatively new technology. This should not be a problem since manufactures try to make this equipment compatible with the existing grid. Moreover, it is expected that the developers of distance protection take care of this new technology.

1.4 Scope

The main purpose of this project is to identify potential problems with the distance protection. This includes changing the simulation to be suitable for electromagnetic transient (EMT), develop a test setup, carry out the test and identify unexpected results. Included in the project is to find the cause of an unexpected result.

1.5 Technical Process

This subchapter describes the steps taken in this project. First, the model is optimized for EMT simulation. After that, a decision is made which scenarios need to be tested. The next step is synthesizing of a part of the simulation in real voltages and currents and testing of the relay. The last step is analysis of the data.

1.5.1 Simulation Model

The software "DigSilent PowerFactory 2018" is used to simulate the grid. Most of the parameters are received from the equipment manufactures. The rest of the parameters are approximated based on literature and common values. Chapter 3 gives a detailed description of the simulation.

1.5.2 Scenarios

A real grid is not static but has fluctuating factors. Especially a wind farm where the generation depends on the wind speed. The grid controller can change the setpoints of the wind turbines (WTs) and the tap setting of the transformer. Faults can occur at various locations, various lines and various fault resistances. 180 scenarios are chosen for testing.

1.5.3 Signal Extraction and Synthesis

The signals at three locations are extracted from the simulation. Each extraction contains the secondary L-G voltages and currents. The power engineering software can export the signals to a file which is readable by an Omicron CMC device. This device can synthesize the voltages and currents. A CMC device was originally developed for calibration of other measurement devices. However, current versions are made for testing of protection relays. Despite the other purpose the acronym CMC is still in use [9].

1.5.4 Test

The voltages and currents are fed into a Siemens Siprotec protection relay. This protection relay will react to these signals like a real grid is connected. The log files and fault records are downloaded from the relay.

1.5.5 Analysis

The most basic feedback from the protection relay is if it will give a trip signal or not. An expectation is given for each test before the test is carried out. The expected options are "trip" or "no trip". There has been looked deeper into each test where the expectation does not match the result of the trip signal and there has been tried to find an explanation for these unexpected results.

1.5.6 Discussion and Conclusion

This report will finish with the conclusion and discussion. It is discussed what part of the project went well, what could be better and next steps to improve. The research questions are answered in the conclusion. This report will be reviewed in the discussion.

Chapter 2

Protection Relay Setup

In this chapter the protection relay and how it is configured for the surrounding grid is discussed. A brief explanation of the internal working is given. Challenges found in literature are described in subchapter 2.3.

2.1 Protection Against Faults

Protection against electrical faults in new medium and high voltage installations is mainly done with numerical protection relays. In addition, specific equipment is protected with Buchholz relays and temperature protection.

A Numerical protection relay is a device that measures currents and/or voltages at one or multiple locations in a power system. It uses these signals in its calculations to determine if there is a fault in the power system. The protection relay can operate a circuit breaker (CB) to interrupt the current when a fault is detected. The method of determination of a fault in the grid is a protection function. The protection functions are discussed in subchapter 2.2.

For this project protection relays are used in the Siemens Siprotec 5 range. The implementation of distance protection differs with other types of protection relays.

2.1.1 Current and Voltage Measurement

In medium and high voltage installations the voltage and current levels are too high to be directly measured by the protection relays. Therefore, current transformers (CTs) and voltage transformers (VTs) are used. Transformers for measurement purposes are also called ITs. These transformers can decrease the voltage so that the nominal secondary voltage is around 100 volt and the nominal secondary current can be around one ampere. These secondary voltages and currents can be fed into the protection relays. Figure 2.1 shows a diagram with an example how the ITs can be setup together with a protection relay.

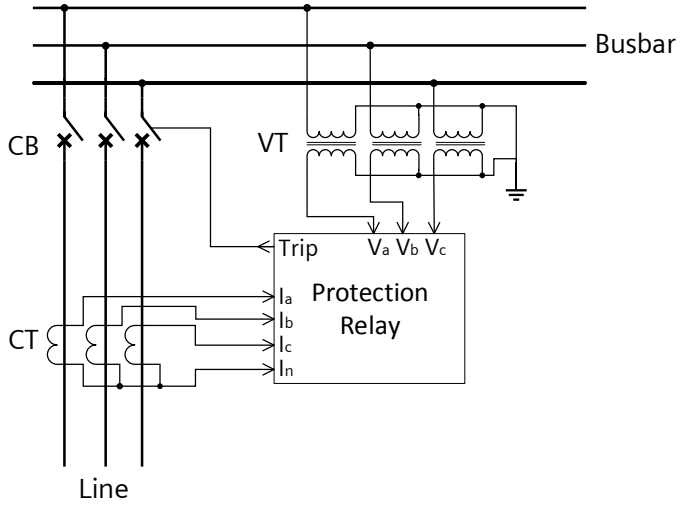

Figure 2.1: Three phase setup of the protection relay.

Like normal transformers saturation is an effect of inductive ITs. In section 3.4.2 can be read how saturation of instrument transformers is considered in this project.

2.2 Fault Detection

The most used protection functions are: overcurrent protection (ANSI 50/51), under and overvoltage protection (ANSI 27/59), differential protection (ANSI 87) and distance protection (ANSI 21). This project is focused on distance protection. Therefore, only this protection function will be discussed.

In the used protection relay two types of distance protection are used. The distance protection with the classic method and the distance protection with the reactance method (RMD). In this project the classic method is used.

2.2.1 Distance Protection

The algorithm behind the distance protection function calculates the complex impedance of a potential fault loop. The impedance is calculated using phasor values of the three-line voltages and three line currents. The three phases (L_A, L_B & L_C) and ground (G) create six loops for current to flow. The currents and voltages are measured by the protection relay at one point in the grid. With these values a loop impedance can be calculated. The equation to calculate these impedances is given in section 2.2.4. Six loop impedances are calculated for the following loops: L_A-G, L_B-G, L_C-G, L_A-L_B, L_B-L_C, L_C-L_A. A small impedance is a sign of a fault. The protection relay will give a trip signal if the impedance is in a preset domain for a preset time. Such a preset two-dimensional domain is called a zone and the preset times are called operate delay. It is common sense to use multiple zones with corresponding operate delays.

2.2.2 Power Direction Determination

For distance protection purposes it is needed to determine the direction of the power. The direction of the current is measured with the phase angle. The phase angle is the angle between the voltage angle and current angle. A phase angle counting from -22° to 122° is default considered as forward. A margin of 23° is set around -45° and 135° which is called the non-operating area defined by the forward angles. Backward is default defined from 158° to -68°.

According to Benitez [10] do these settings of degrees not always hold. For example, in a network with a high capacitance or high inductance. Therefore, the networks must be reviewed, and the settings need to be adjusted to the network. The method of Jaramillo [11] can help with the determination of the settings. The most critical situation is when there is a low current flowing through the CT. In this situation the sensitivity of the current and voltage measurement plays an important role.

The direction depends on the connection of the CT. A CT is connected star configuration. The neutral point can be connected at the busbar side or the side of the object to protect. Most common is to connect the neutral point at the object to protect. Figure 2.1 shows the latter configuration. In the configuration of figure 2.1 is forward defined in the direction of the line.

2.2.3 Zone Setting

The zones are programmed in the relay. Multiple shapes are possible to form the domain. However, in this project only a quadrilateral shape is used. The use of quadrilateral shapes are an requirement of the client. This is because the have to match the shapes in neighboring areas. Moreover, a quadrilateral shape is advised over an MHO-shape. A quadrilateral can better be matched to the protected line because Xreach and Rreach are independent. This has as an advantage that Xreach can be set very tight to X of the zone and Rreach can be set to compensate for the arc resistance. The quadrilateral shape is defined by a couple of parameters. Figure 2.2 shows how the quadrilateral is constructed using these parameters.

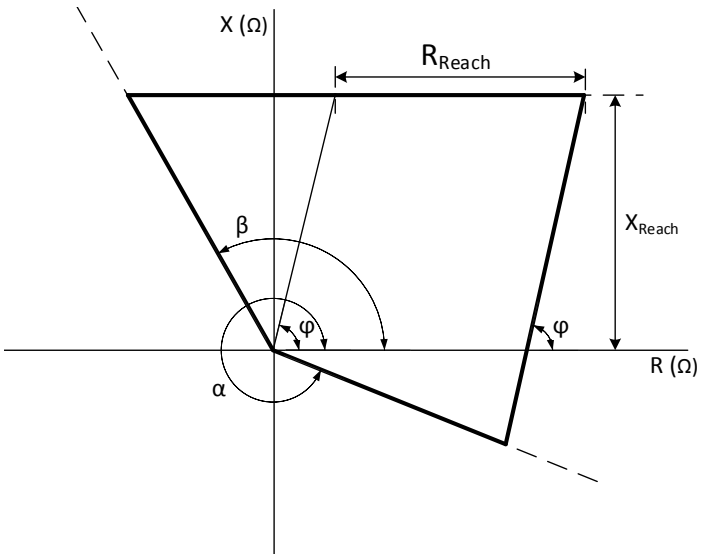

Figure 2.2: The relation between the zone-parameters and the quadrilateral shape.

The involved parameters are:

- Distance characteristic angle: the angle of the reactance and resistance of the protected equipment calculated with

$$\varphi = arctan(\frac{X_l}{R_l}). \tag{2.1}$$

- Forward angle α and β which are defined by default as $\alpha = 338^\circ$ and $\beta = 122^\circ$.
- R_{reach} sets the maximum resistance at $X = 0$.
- X_{reach} sets the maximum reactance of quadrilateral
- Direction (Forward/Reverse), Reverse will rotate the quadrilateral with 180° around the origin.

2.2.4 Impedance Calculation

Two different equations are used to determine the loop impedances. These equations can be found in the Siprotec 5 manual [12]. For the line to line impedances ($L_A - L_B$, $L_B - L_C$, $L_C - L_A$) the following equation is used:

$$\underline{Z}_{L_A - L_B} = \frac{\underline{U}_{L_A - G} - \underline{U}_{L_B - G}}{\underline{I}_{L_A} - \underline{I}_{L_B}} \tag{2.2}$$

Where:

$\underline{U}_{L_A}$ and $\underline{U}_{L_B}$:	Voltage phasors of the considered lines.
$\underline{I}_{L_A}$ and $\underline{I}_{L_B}$:	Current phasors of the considered lines.

The earth impedance is different from the line impedance. This makes the L-G impedance calculation more advanced. Therefore, the ratio between impedance of the earth path and the line impedance is included in the equation. This ratio is a complex number and is called the residual compensation factor (RCF) and is designated as:

$$\underline{k} = k_r + k_x\, j = \frac{R_G}{R_L} + \frac{X_G}{X_L}\, j \tag{2.3}$$

The L-G resistance and reactance can be calculated with the following equation using phasors:

$$R_{L-G} = \frac{|U_{L-G}|}{|I_L|} * \frac{cos(\varphi_U - \varphi_{I_L}) - \frac{|I_G|}{|I_L|} * k_X * cos(\varphi_U - \varphi_{I_G})}{1 - (k_X + k_R) * \frac{|I_G|}{|I_L|} * cos(\varphi_{I_G} - \varphi_{I_L}) + k_R * k_X * (\frac{|I_G|}{|I_L|})^2} \tag{2.4}$$

$$X_{L-G} = \frac{|U_{L-G}|}{|I_L|} * \frac{sin(\varphi_U - \varphi_{I_L}) - \frac{|I_G|}{|I_L|} * k_R * sin(\varphi_U - \varphi_{I_G})}{1 - (k_X + k_R) * \frac{|I_G|}{|I_L|} * cos(\varphi_{I_G} - \varphi_{I_L}) + k_R * k_X * (\frac{|I_G|}{|I_L|})^2} \tag{2.5}$$

Where:

$\lvert U_{L-G}\rvert$:	RMS value of the fundamental phase A to ground voltage frequency component
φ_U:	Angle of the phase to ground voltage
$\lvert I_L\rvert$:	RMS value of the fundamental phase current frequency component
φ_{I_L}:	Angle of the phase current
$\lvert I_E\rvert$:	RMS value of the fundamental earth current frequency component
φ_{I_G}:	Angle of the ground current

2.2.5 Signal Processing

The analog voltages and currents are digitized with a sample rate of 16 000 samples per second [12]. The values used for the distance protection function is determined at 1 kHz. These values are calculated using the previous cycle. This means for 50 Hz that the previous 20 samples are used [13].

2.2.6 Filtering

A digital filter is used to filter the incoming voltage and current samples. The filter is used to remove unwanted oscillations from the grid and side effects of the instrument transformers [13]. During the operation a finite impulse response (FIR) filter is used. A filter is mainly important during transients where higher frequencies are sampled. The filter coefficients are a trade-off between measurement of distortions and detail [14]. The purpose of the filter is to keep only the fundamental frequency component of the signal (around 50 Hz in Europe). The filter parameters used in the protection relay is unknown. Digital filters can be placed at different steps in the signal processing chain.

Decision tree

The distance protection with the classic method uses a decision tree to decide which calculation method is used. Examples of decisions in this decision tree are: forward or reverse, use the actual voltages or the memory voltage. The design tree of the classic method is hierarchical. Therefore, if one decision is made it does not consider the other calculation methods. In this project is the distance protection with the classic method used.

The RMD distance protection function uses a flat decision tree with weighted factors. Therefore, it does always consider all calculation methods.

2.3 Challenges in Protection

It has been found that the challenge of protection is higher in some situations. Literature has been consulted to find these situations [6, 7, 13, 15]. In this subchapter are some challenges discussed. Some of the situations listed below are only a concern for generators with PEC. Others are also applicable for directly connected generators.

Large fault resistance

One malfunction of the distance relay can be caused by a large fault resistance. An example of this fault resistance is an arc [6]. Distance protection measures the impedance. A fault is often characterized by its low impedance. However, an arc has resistive impedance. This arc-resistance can be of significant value in air insulated parts of the grid. If this fault impedance is high enough the fault could not be detected or is calculated in the incorrect zone.

Low energy production

The energy generation in a wind farm is not always high. When the RES produces a low amount of energy, a fault could be hard to detect for measurements at the RES side of the grid. This is because the fault current is low. Therefore, the measured impedance will stay high. Three phase and single-phase to ground faults could stay undetected [6, 15].

Transients

Voltage and current measurements during a transient are a challenge. DC- and frequency -components higher than the grid frequency are present during a transient. A filter is used to find the power frequency component. A Fourier based algorithm can be used to filter the power frequency component. This detection can be inaccurate during transients according to Li et.al. [15]. Unfortunately, paper does not give the reason for unreliable results from the Fourier algorithm.

Transformers

Distance protection is not often used as primary protection for a transformer. It can be used as back-up protection. A distance measurement can measure through a transformer. Some characteristics need extra attention if measured through a transformer. Impedances seen from the other side of the transformer appear as another value dependent on the transformer ratio. The angle is also changed if a star/delta transformer is used.

The two sides of autotransformers are electrically connected. The change impedance has as effect that the RCF needs to be set differently. A calculation is given in the book of Ziegler [13]. For this calculation a positive negative and zero- sequence network needs to be found.

Crowbar

Type 3 WTs contain a crowbar circuit. An incorrect measurement in the distance protection can occur when the crowbar circuit is operated. The generator current is limited when the crowbar circuit is in operation. A protection relay may not detect the fault if the current is low. The impedance angle can change due to the crowbar resistances. According to research of Rijcke [6] has this phenomenon only an influence on the detection of three phase and single-phase faults. An detailed explanation of a type 3 wind turbine is given in section 3.4.1.

Chapter 3

Description of the study case network

In this chapter first, a description is given of the wind farm transport grid considered in this project. In the second part of this chapter the consideration is described between different calculation methods. Detailed information about the modeling of the grid is described in subchapter 3.4.

3.1 General Overview of the Grid

Figure 3.1 shows a simplified single line diagram (SLD) of the grid considered in this project. This grid connects the wind turbines to the main transmission grid. Fault locations and protection relays are also visible in this diagram. The grid is elaborated in this subchapter. The main parts are discussed from top to bottom.

Note that figure 3.1 does show a simplified version of the grid used in this project. This grid differs from the real wind farm grid build in the North Sea.

External grid

The grid is connected to the main transmission grid at the 380 kV bus. The transmission grid is simplified by using a synchronous machine model. Two sets of parameters are used to denote the utmost conditions. The situation with the lowest series impedance is denoted as strong grid or maximum short circuit condition. The situation with the highest series impedance is denoted as weak grid or minimum short circuit condition.

- Maximum external grid strength: Short circuit Power of 25 GVA, Short circuit current of 38 kA
- Minimum external grid strength: Short circuit Power of 7.1 GVA, short circuit current 10.8 kA.

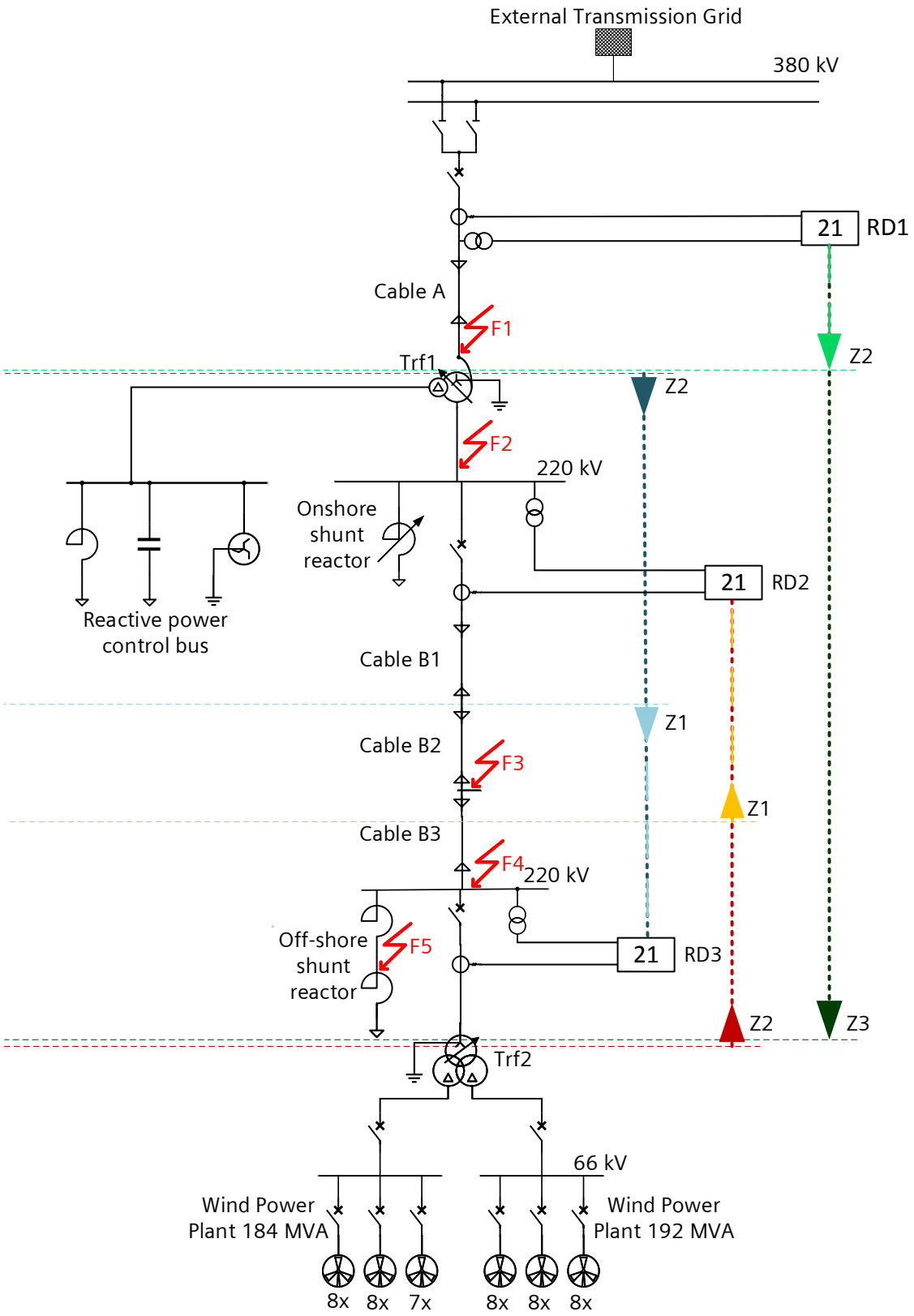

Figure 3.1: Simplified overview of the wind farm grid as modeled including fault locations.

Distance protection relay 1

The distance protection relay 1 (RD1) is connected to a CT (figure 3.2a) and a VT (figure 3.2b). The arrow in figure 3.1 denotes the forward direction of the relay. This set of equipment is connected as shown in figure 2.1. Section 2.2.1 gives more details about the protection relay configuration. Section 3.4.2 elaborates on the topic of saturation in the ITs.

(a) (b)

Figure 3.2: Single line diagram symbol of a current transformer 3.2a and voltage transformer 3.2b.

Cable A

Cable A is a ground cable with a length of 350 m. This cable is modeled as a Pi-section. Section 3.4.3 elaborates on this choice of modeling.

Transformer 1

Transformer 1 (Trf 1) is a three winding transformer which is in autotransformer configuration in the primary to secondary side. The tertiary side of a transformer is galvanically isolated. The nominal voltages of the windings are as follows: Primary 380 kV, secondary 225 kV and tertiary 33 kV. The star point is grounded. The voltage ratio can vary since there is a tap-changer at the primary side. This tap changer can change the number of turns from 85 % to 115 % in 20 taps.

Reactive power control bus

The tertiary side of transformer 'Trf 1' is connected to a 33 kV reactive power control bus. A shunt reactor, capacitor bank and earthing transformer are connected to this bus. The shunt reactor has a fixed absorption of 65 Mvar (at nominal bus voltage). The capacitor bank has a fixed injection of 32.5 Mvar (at nominal voltage). These can be turned on and off.

Distance protection relay 2

Distance protection relay 2 (RD2) measures at terminals of the secondary side of transformer 'Trf 1'. The forward direction points towards transformer 'Trf 1'. However, the zones are set as backward. This means that RD2 should trip at a fault in cable B and not in transformer 'Trf 1'.

Onshore shunt reactor

The onshore shunt reactor has a variable absorption of 52 to 130 Mvar in 33 taps. The star point of the shunt reactor is connected to earth.

Cable B

The composed cable B is a submarine cable and is at one side connected to the on-shore substation and at the other side to the off-shore platform. The first section (cable B1) is 16 km long and has different properties as the second section (cable B2). The cable B2 is 14 km long and has equal properties as the third section (cable B3) which is 30 km long. The division between cable B2 and B3 is only made in the simulation to be used as fault location and does not exist in the real system. The cable is modeled with the distributed parameter method. The end of the cable is terminated to the bus at the off-shore platform.

Off-shore shunt reactor

The offshore shunt reactor has a fixed absorption of 76 MVar. The reactor is split into two parts to model a fault in the windings. One part is modeled as a series reactor, the other part is modeled as a parallel reactor. Both absorbing 38 MVar. More about this configuration can be read in section 3.4.2.

Distance protection relay 3

Distance protection relay 3 (RD3) is connected to a CT measuring at the terminals of transformer 2 'Trf 2'. The CT is connected with the neutral side to transformer 'transformer 2 (Trf 2)', this means that the forward is defined in the direction of transformer 'Trf 2'. The zones are set as backward and therefore cable B is protected.

Transformer 2

Transformer 2 (Trf 2) is a three winding transformer connected on the primary side at the 220 kV platform bus. The secondary and tertiary side are both connected to a 66-kV WPP bus.

Wind Power Plants (WPP1 & WPP2)

WPPs work at 66 kV. WPP1 has 24 wind turbines evenly divided over three strings. WPP2 has 23 wind turbines divided over three strings. Each string is connected to a cable of 15 km. This cable is modeled as two Pi-sections in series.

Wind turbines

The wind turbines (WTs) are type 3 based on a doubly fed induction generator (DFIG). Each wind turbine has a nominal power of 8 MVA. The reactive power of the wind turbines is set differently for each scenario. It takes a lot of computational resources to model all the wind turbines separately. Therefore, multiple WTs in a string are merged together into one large aggregated WT model. This method is described in an paper: "Wind Farm Electromagnetic Dynamic Model and Outgoing Line Protection Relay RTDS Testing" [15]. This method has been validated and no difference can be found between the separate and merged WTs. A detailed description of the wind turbine model can be found in section 3.4.1.

3.2 Faults

The fault locations are chosen at a location where it is likely that faults occur and/or where faults are expected. The locations of the faults are listed in table 3.1 and can also be found in figure 3.1.

Table 3.1: Location of the faults in the simulation.

Fault name	Location description
F1	At the 380 kV terminals of transformer T1
F2	At the CB which connects cable B to the grid
F3	At 50 % of the length of cable B
F4	At the 220 kV offshore bus
F5	Inside the off-shore reactor, at 50 % of the windings

3.2.1 Fault Resistance

A fault can initiate an arc which has a resistance. Fault locations F1 and F2 are located at an air insulated substation. If a fault occurs at these locations it is likely that an arc is initiated. Therefore, the scenarios with fault locations F1 and F2 are simulated with and without a fault resistance.

The fault resistances are different for each location and each type of fault. There has been looked at the geometry of the equipment. The clearance distance has been taken as arc length l_{arc}. The arc resistance R_{arc} is calculated using the following equation:

$$R_{arc} = \frac{E * l_{arc}}{I_{arc}} \tag{3.1}$$

Where I_{arc} is the fault current and E a constant of 2500 [16]. To create the worst-case scenario the minimum short circuit current is chosen to be the fault current. Table 3.2 gives the arc length and minimum short circuit current for different types of faults at locations F1 and F2.

Table 3.2: Arc Resistance, minimum short circuit current and arc length for different types of faults at locations F1 and F2.

Fault location	Fault type	Arc length l_{arc} (m)	Minimum short circuit current I_{arc} (kA)	Arc resistance R_{arc} (Ω)
F1	L-G	5.7	9.3	2.25
F1	L-L-G	5.7	9.3	2.25
F1	L-L	5.5	10.8	2
F1	L-L-L	5.5	10.8	2
F2	L-G	2.8	8.5	1.2
F2	L-L-G	2.8	8.5	1.2
F2	L-L	2.8	5.2	1.7
F2	L-L-L	2.8	5.2	1.7

A fault at F3, F4 and F5 has no or only a small fault resistance in case of a fault. Therefore, a fault resistance of 0 Ω is used. The fault model used in this project only uses the arc impedance. Therefore, the fault impedance is equal to the arc impedance ($R_f = R_{arc}$)

A fault with fault resistance is modeled as a resistance between lines or between a line and ground. The configurations for a L-L, L-L-G and L-L-L fault can be seen in figure 3.3.

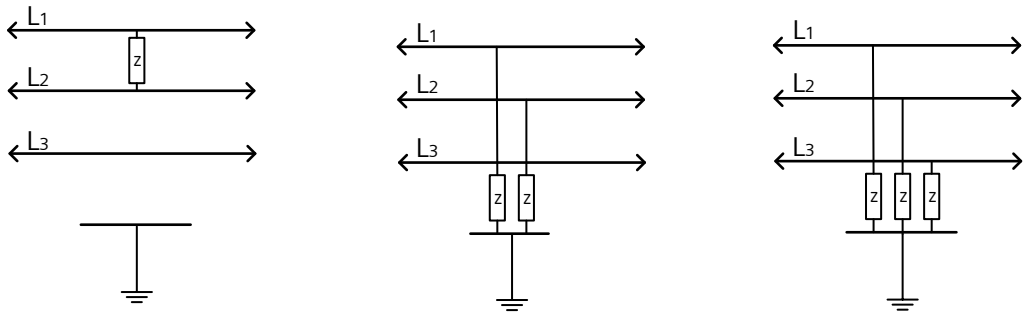

(a) (b) (c)

Figure 3.3: Configurations of modeling a fault resistance for a L-L fault (3.3a) a L-L-G fault (3.3b) and a L-L-L fault (3.3c).

Wind

The length of an arc in open air can increase over time by wind. This property is not taken into account in this simulation.

3.3 Testing and Modeling Methods

Testing in real power systems is not often an option because of the high value of the equipment. However, a power system must function correctly because many parties depend on it. Models are made to approximate the real-world situation. With these models a confident decision can be made on the design. Multiple types of modeling are highlighted in this subchapter: analytical model, full simulation and partly simulation

3.3.1 Analytical Model

An analytical model uses algebra to model a power system. Equations are used from the known theories for example from Gauss and/or Kirchhoff. These equations are used for this system. An analytical model can give a deep insight into a model. However, it asks more time and skills than other options for modeling [17].

3.3.2 Full Simulation

A simulation which is fully executed on a computer has the advantage that it is very flexible. Software such as DIgSILENT PowerFactory or Siemens PSS/e is special programmed for Power systems simulation [18]. Simulated time in this kind of software is independent of the real time. Equations are numerically solved. A disadvantage is that human mistakes or imperfections can easily stay undetected and real equipment can differ from the simulation.

3.3.3 Partly simulation with Real Equipment Testing

In this project a variation of the full simulation is used. Part of the tests are carried out using real equipment. The simulation calculates all values for all the modeled equipment. The voltage and current values for the real equipment are synthesized with a digital to analog converter. The equipment operates like it is in a normal grid. This type of modeling is very suitable for protection relay testing [19]. Protection relays are relatively easy to transport and complex to model in software. Since the algorithms applied in this equipment is not available for other parties. Therefore, this will give a more accurate result than a full simulation.

3.4 Grid Model

This subchapter describes the model as simulated in "DigSilent PowerFactory 2018". Not the whole simulation is made in this project. A static model of the grid is profited. This model is modified to be suitable for EMT simulations. Important modifications are saturation of the transformers, cable model and the wind turbines.

3.4.1 Wind Turbine Model

WTs are categorized in four types depending on their connection to the grid. Type 3 and type 4 WTs make use of a PEC. PECs work as follows: In a first step the electric power is converted from DC or AC with a frequency different than the grid frequency. The PEC converts the electric power so that it is synchronized with the grid. Power electronics have limitations because of thermal properties of the semiconductors [20]. One of these limitations is the short circuit current which is limited compared to a synchronous generator. A lower short circuit current makes the detection and isolation of faults more difficult.

A full PEC WT is called a type 4 WT. A PEC is placed between the generator and the grid connection. The rotor and generator rotate at a speed different from the grid. The PEC converts all the power produced by the generator. These types of wind turbines have a very low short circuit ratio (SCR), with typical values of 1.1 [21].

Doubly Fed Induction Generators

A type 3 WT is used in this project. A DFIG is a type of electrical machine. In this type of machine the rotor winding is connected to a power electronic converter. A correct control of the PEC can set the stator frequency equal to the grid frequency with a varying shaft frequency. This type of generator was the common in large WTs in 2011 [15]. Figure 3.4 shows a general layout of a WT on a DFIG basis.

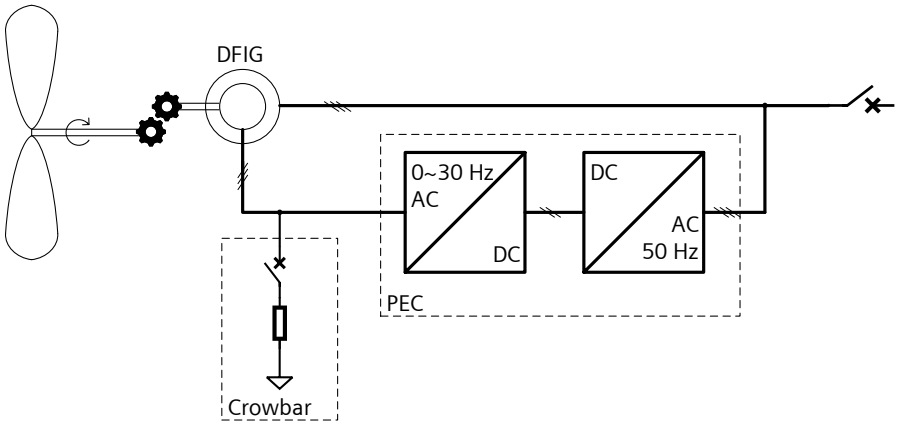

Figure 3.4: Schematic diagram of a type 3 (DFIG) wind turbine.

In most types of type 3 WTs the converter is protected against overloading with a crowbar circuit. This is a circuit with resistors where the excess energy is dissipated in case of high current through the PECs.

Often a chopper system is used on the DC side on the PEC. This chopper can be controlled to reduce the rotor current.

Modeling of the wind turbine

Multiple standard WTs models are considered to be used in the simulation, including WECC [22] and IEC 61400-27-1 [23] based models. The DigSilent wind turbine generator (WTG) template model [24] is chosen because of the compatibility with EMT simulations and possibility to examine and change the full model. The following section describes the DigSilent WTG model in general.

General description of the WT control Model

The DFIG generator works at a voltage of 690 V. Each wind turbine has its own transformer which transforms the voltage to 66 kV. The PEC and crowbar control are modeled in a control system. A simplified control loop is given in figure 3.5.

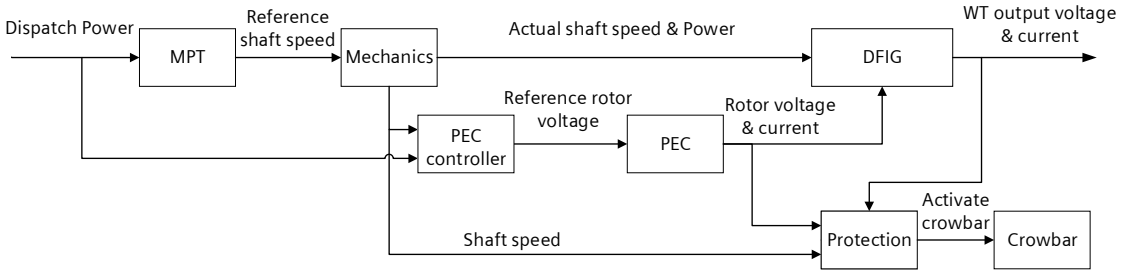

Figure 3.5: Simplified control loop of the DigSilent WTG model.

In contrast to the real world, not the wind speed but dispatch power is used as input. A maximum power tracker (MPT) calculates reference shaft speed. This reference shaft speed is used as input for the mechanical model.

The mechanical model includes the rotor pitch controller, turbine model and shaft model. The angle of the rotor blades is set by the rotor pitch controller. The turbine model calculates the actual output power using the wind speed, rotor angle and the shaft speed. The shaft model translates this power in a actual shaft speed and actual shaft power.

In the PEC controller the output voltage and current are transformed into the direct-quadrature (dq) domain. These dq values can be used in a proportional-integral controller (PI-controller) to determine the needed rotor voltages. A reference signal is sent to the PEC which converts the correct voltages for the rotor.

WTs use a couple of internal protection functions. "Over frequency" reduces the power if the electrical frequency is higher than a setpoint. Other protection functions are:

- Shaft overspeed
- Shaft underspeed
- Stator overvoltage
- Stator undervoltage
- Rotor overcurrent

These protection functions can activate the crowbar or disconnect the WT to stabilize the grid and protect the internal components.

3.4.2 Transformers and reactors

The grid consists of multiple types of equipment with windings for example power transformers, reactors, current transformers and voltage transformers. Electrical machines are not considered in this section. This type of equipment has the property to saturate.

Saturation

The magnetizing inductance of a transformer is assumed to be stable if the voltage is equal or lower than the nominal value. At higher voltages the core saturates with flux. When this happens the ratio between flux and current is not linear. For the transformers and reactors in the grid the ratio between flux and current is not given but the peak and knee current are supplied. A method is given by CIGRE [25] to calculate the saturation characteristic given the knee point and peak current. This method is used to approximate the saturation characteristics.

Fault modeling in a shunt reactor

The effect of an internal fault inside a shunt reactor on the distance protection is investigated. A fault is modeled inside the windings of the off-shore shunt reactor. The shunt reactor is split into two parts, one series reactor and one shunt reactor. Both absorb 50 % of what the single reactor would absorb. With this method a fault can be modeled at 50 % of the windings. This will mimic a short circuit between turns or between a turn and the core of the reactor. Scenarios with L-L, L-G, L-L-G and L-L-L faults are tested.

Is has been checked if the behavior of the single shunt reactor is almost equal to the spitted shunt reactor. The input parameter of the series resistance is altered to get an almost equal response.
A single reactor model is used for the tests when no fault is initiated inside the reactor.

Instrument transformers

The CTs and VTs transform the current and voltages so that it is low enough to be measured by the protection relay. The transformer ratios are listed in table 3.3. The secondary side is connected to the protection relay.

Table 3.3: Ratios of the ITs.

Connected Protection Relay	CT or VT	Primary	Secondary
RD1	CT	1000 A	1 A
RD1	VT	$380/\sqrt{3}$ kV	$100/\sqrt{3}$ V
RD2	CT	1250 A	1 A
RD2	VT	$220/\sqrt{3}$ kV	$110/\sqrt{3}$ V
RD3	CT	1250 A	1 A
RD3	VT	$220/\sqrt{3}$ kV	$110/\sqrt{3}$ V

3.4.3 Cables

Special attention is needed for modeling long cables. An impedance in series and parallel is the effect of the interaction between the metals and dielectrics in the cables. These characteristics let the cable act as a filter. There are multiple ways to model these characteristics in a cable. Sort cables are typically modeled with lumped elements in Pi-configuration. This method can be extended to place multiple Pi-sections in series. For longer cables the accurate method of distributed parameter is recommended.

Definition short and long cables

The wavelenth (λ) of the signal determine if the length of the cable (l) is considered long. The following rule of thumb is given in the book of Ulaby[26]: *"When l/λ is very small, transmission-line effects may be ignored, but when $l/\lambda \lessapprox 0.01$, it may be necessary to account for the phase shift due to the line delay."*. The protection relay samples at 1 kHz. In the following example is checked if cable section B2 can be considered as long or short cable. The protection relay has a sample frequency of 1000 Hz. The highest detectable frequency (f) is 500 Hz using the Nyquist criterion [27]. λ can be calculated using the following equation:

$$\lambda = \frac{1}{f * \sqrt{L'C'}} \tag{3.2}$$

where L' is the series inductance per km and C' is the parallel capacitance per km.

The parameters for cable section B2 are:

- $C' = 0.196 \quad \mu F/km$
- $L' = 0.369 \quad mH/km$
- $l = 14 \quad km$

This evaluated using equation 3.2 gives $\lambda = 235$ km. Thus, $l/\lambda \approx 0.060 > 0.01$. Therefore, transmission line effects cannot be ignored, and this cable section should be considered as a long cable.

Lumped element Pi-model

A short cable can be modeled with lumped elements in a Pi-configuration. Figure 3.6 shows a Pi-configuration with the series inductance Z and the parallel susceptance Y.

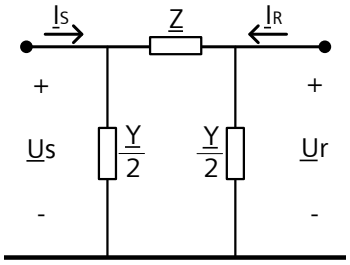

Figure 3.6: A cable can be modeled with an impedance in series and two in parallel.

$\underline{Z}$ consists of a resistance and inductance. $\underline{Y}$ consists of a capacitance and resistance. The parallel resistance is often neglected because it is very large relative to the other characteristics. A Pi-section can be seen as a second order filter. The disadvantage of this model is that the real susceptance is not only at the beginning and the end of the cable but distributed over the whole cable. Every cable in the grid is modeled with one Pi-section except for cable B.

It is possible to model a cable with multiple Pi-sections in series. More Pi-sections in series means a better accuracy.

Distributed parameter

A formula can be created by mathematicly adding an infinite number of pi-sections in series. The transfer functions are derived from the principle that the impedances are distributed over the total length of the cable. The method for these calculations is called the Bergeron's Method described in the book of Meyer [28]. The Bergeron's Method uses a model of two voltage sources in series with a surge impedance $\underline{Z}_C$. Figure 3.7 shows the circuit used for the distributed parameter method.

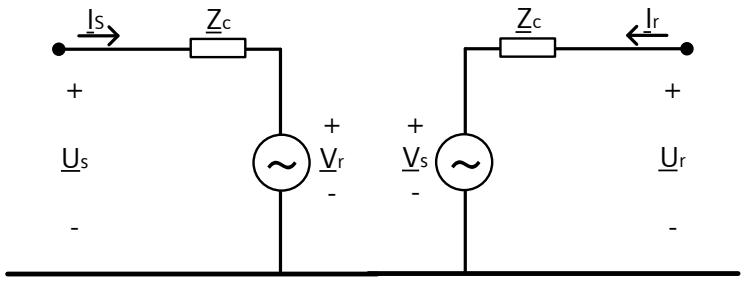

Figure 3.7: Distributed parameter model using the Bergeron method.

The following calculation can be done to find the voltages and currents at the receiving end if the voltages and currents at the sending end are known.

$$\underline{U}_r = (\frac{\underline{U}_s - \underline{I}_s \cdot \underline{Z}_c(\omega)}{2}) \cdot e^{\underline{\gamma}(\omega) \cdot l} + (\frac{\underline{U}_s - \underline{I}_s \cdot \underline{Z}_C(\omega)}{2}) \cdot e^{-\underline{\gamma}(\omega) \cdot l} \tag{3.3}$$

$$\underline{I}_r = (\frac{\underline{U}_s - \underline{I}_s \cdot \underline{Z}_c(\omega)}{2 \cdot \underline{Z}_c(\omega)}) \cdot e^{\underline{\gamma}(\omega) \cdot l} - (\frac{\underline{U}_s - \underline{I}_s \cdot \underline{Z}_C(\omega)}{2 \cdot \underline{Z}_c(\omega)}) \cdot e^{-\underline{\gamma}(\omega) \cdot l} \tag{3.4}$$

$\underline{Z}_c$ and the propagation factor $\underline{\gamma}$ are functions of ω.

$$\underline{Z}_C(\omega) = \sqrt{\frac{R' + j\omega L'}{G' + j\omega C'}} \tag{3.5}$$

$$\underline{\gamma}(\omega) = \sqrt{(R' + j\omega L') \cdot (G' + j\omega C')} \tag{3.6}$$

Validation

A consideration is made between the different methods of cable modeling. A Pi-section is the simplest model, multiple Pi-sections makes it a bit more accurate, but the distributed parameter is even more accurate. A separate model is made in Digsilent PowerFactory and Matlab Simulink to compare the different cable models.

The properties of cable section B-3 are used as input. The first configuration consists of a single Pi-section. The second and third configurations have respectively 8 Pi-sections and 16 Pi-sections. The fourth cable has a distributed parameter model. Figure 3.8 shows the impedance characteristic which is calculated for a frequency from 0 to 1 kHz. This cable shows the frequency response from the cable B-3 in PowerFactory. The four configurations are very similar for frequencies lower than 500 Hz. Above this frequency can be seen that the higher the number of Pi-sections the closer the characteristic approximates the distributed parameter.

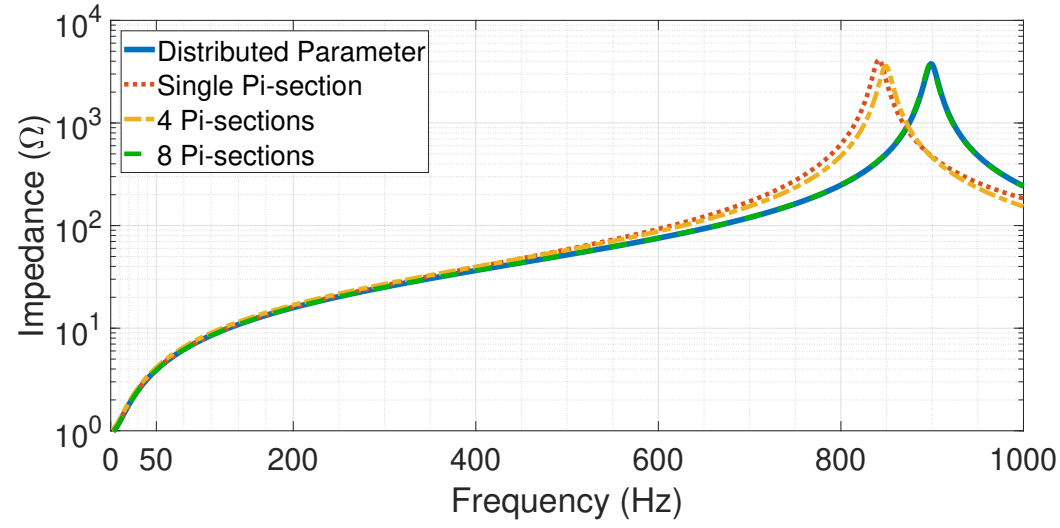

(a)

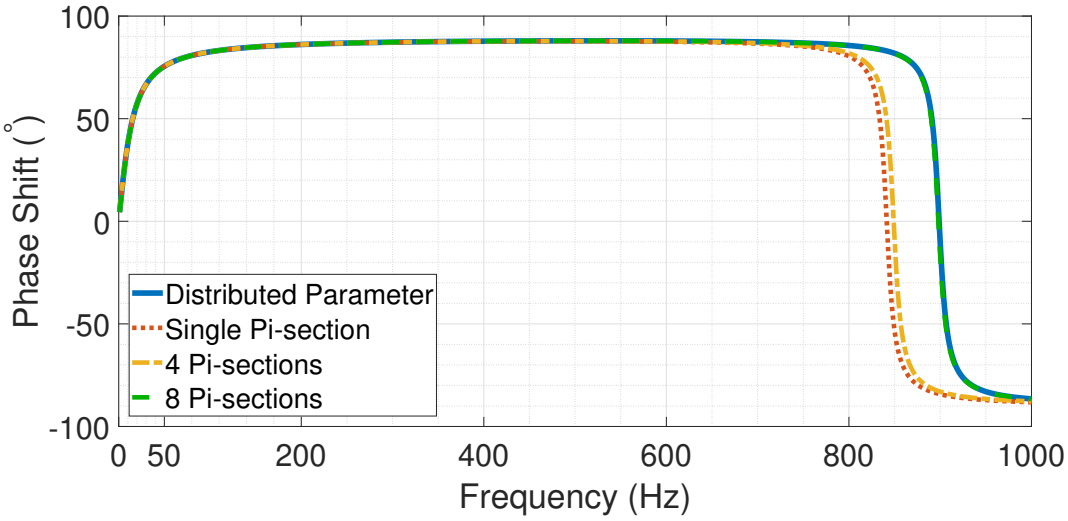

(b)

Figure 3.8: Frequency response (3.8a) and phase resoponce (3.8b) of four cable model configurations.

Most of the energy has a frequency of 50 Hz in normal operation. Nevertheless, there is chosen for a distributed parameter model for all sections of cable B because a resonance can occur in the higher frequencies. This resonance could form a problem in protection. Section 2.2.6 describes that the protection relay uses a filter. Higher frequency resonances could stay undetected for the protection relay due to this filter and the limited sample rate.

A comparison is made between the distributed parameter model and the Pi-model. A fault is initiated at F2. The simulation results at RD3 are analyzed. First, the distributed parameter model is used for cable B. After that a pi-model is used. The difference can be seen in figure 3.9. The figure shows two L-G and two L-L reactance waveforms. One reactance waveform is the result of a model with a distributed parameter for cable B, the other of a model with all pi-sections. The signals are not filtered to make higher frequency components visible. The signals differ in the transient but converge to a steady state difference of around 0.3 %.

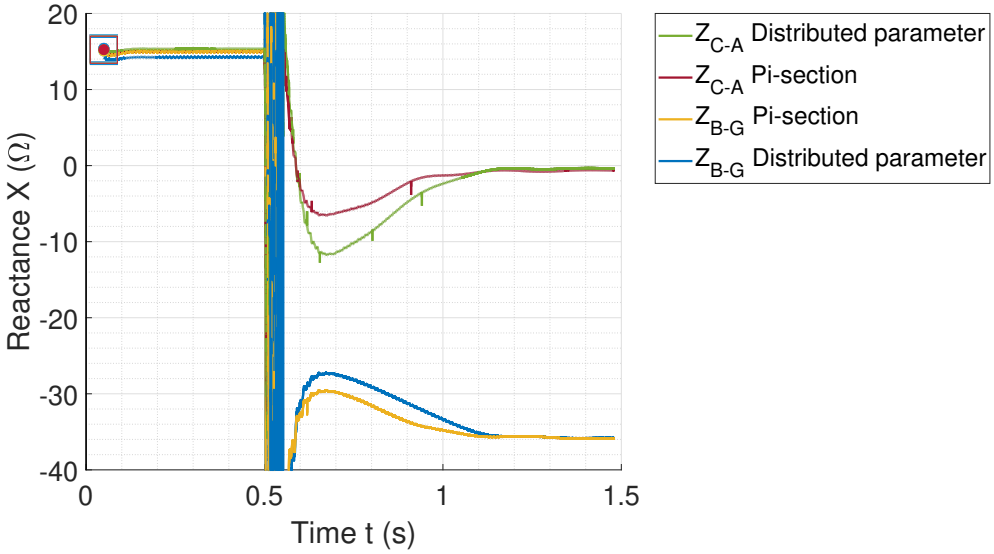

Figure 3.9: Example of a unfiltered L-G and L-L reactance over time with a fault initiated at 0.5 s with two cable models.

3.5 Distance Protection Settings

The distance protection zones are set to protect a certain area of the grid. The dashed lines in figure 3.1 denote the protected zones. The arrow pointing towards the relay means that the zone is set in reverse direction. The arrows pointing away from the protection relay means the zone is set in forward direction. The impedance of the protected equipment is calculated. The parameters to form a quadrilateral shape are listed in table 3.4. Section 2.2.3 shows how the quadrilateral is constructed using these parameters. Table 3.4 shows the secondary settings. The smallest zone in protection relay RD1 is "Zone 2".

Table 3.4: Distance zone settings for protection relays RD1, RD2 and RD3.

Setting	RD1 Zone 2	RD1 Zone 3	RD2 Zone 1	RD2 Zone 2	RD3 Zone 1	RD3 Zone 2
Distance Characteristic angle (φ)	90°	90°	76.8°	76.8°	76.8°	76.8°
R_{reach} (Ω)	4.55	19.29	3.67	13	3.67	8.1
X_{reach} (Ω)	4.55	19.29	3.67	13	3.67	8.1
Direction	Forward	Forward	Reverse	Reverse	Reverse	Reverse
Operate delay (s)	0.23	0.44	0	0.23	0 s	0.23 s

Chapter 4

Simulation and Test

In this chapter the procedure is described how the simulations and tests are carried out. A grid model is optimized for EMT simulations. Several scenarios have been selected to be simulated. Secondary values of the ITs are extracted and synthesized to be fed into the protection relay. The records from the protection relay are downloaded to the PC.

Make the model

A basic model of the grid is given. This model is expanded so that it can be used for EMT simulations. The results of the simulation are checked on unrealistic values. Some small calculations are done by hand to check specific values.

Define scenarios

A list is made of all possible scenarios which arise when parameters are varied. The varied parameters are given in table 4.1. From all possible scenarios 180 scenarios are selected which will be tested. Only the most critical scenarios are simulated. Subchapter 2.3 describes some of these scenarios. Besides those scenarios, also some extreme scenarios are selected.

Subchapter 4.2 describes the process of using this list as a basis for a database which contains all variable settings and pointers to results.

Table 4.1: Scenario dependent equipment settings.

Parameter	Range
Reactive power setpoint per Wind turbine	-0.546 - 0.36 MVar
Tap position offshore transformer	tap 8 - 10
Tap position onshore shunt reactor	tap 40 - 65
Reactor 33 kV	connected/disconnected
Capacitor 33 kV	connected/disconnected

Simulation and extraction of Signals

There has been chosen to simulate 1.5 seconds for every scenario. In every scenario a disturbance is initiated at 0.5 seconds. A disturbance can be a fault, switching action or another event in the grid. The disturbance is present for one second. The feedback from the protection relay has no influence on the course of the fault.

For each selected scenario and each protection relay (RD1, RD2 & RD3) the three L-G voltages and L-G currents are exported to a "comtrade" file. Subchapter 4.2 describes the method of extracting the signals.

Test setup

Build the test setup with the CMC and the protection relay. This includes programming the protection relay.

Run the test

The tests are carried out as described in subchapter 4.3.

Gather and process data

The data received from the tests are stored in a structured way. The location of useful data is stored in the database.

Analysis

For every scenario is checked if a trip signal from the protection relay is expected. The recorded signal is analyzed if the expectation differs from the real signal. Every unexpected result is categorized in a group with a similar behavior.

4.1 Data Management

All the grid scenarios are listed. This list is the basis for a database. This database connects every scenario to the correct operating points and keeps track of the test data. Another function of the database is to generate a script which can be used to control the PowerFactory simulation.

4.1.1 Power Dependent Grid Settings

Some settings of devices in the grid depend on the level generated power from the WTs. In the real grid these settings are controlled by the grid controller. However, the time span for this simulation is only 1.5 seconds. The grid controller has a much longer control time. Therefore, for each simulation only a static value is used per scenario. No dynamic grid controller is included in the simulation. Table 4.1 shows the values which vary for different scenarios. Every level of power can be used for the simulation. However, to reduce complexity only 0, 10, 70 and 100% of power generation levels is used. This corresponds with 0, 0.8, 5.6 and 8 MW of generation per WT.

The power levels and their matching equipment settings are added into a table in the database.

4.1.2 Comtrade File Format

During this project the Comtrade file format is chosen to be the default for saving sampled signals. This file format is used in two ways. The signals generated from the simulation are exported to a comtrade format. Secondly is comtrade the main file format for the protection relay to save the recorded signals.

The comtrade format has a minimum of two files, the *.cfg file with the configuration and a *.dat file with the actual signal sample data. Extra files can be added such as *.rio where the protection relay settings are saved.

4.2 Simulation Automation

Simulating the behavior for 1.5 seconds takes around 100 seconds of computation time for the PC. It would be time inefficient to manually set all the values and start each simulation by hand. Therefore, this part is automated so that the PC can run for a couple of hours and simulate without any human input in between.

4.2.1 Script

In the database can be selected which scenarios needs to be simulated during this run. A query in the database is used to generate a DPL script. DPL stands for "DigSilent Programming Language" which can control almost every function in DigSilent PowerFactory. The generated script sets all the varying settings for each scenario and automatically runs the simulations one after the other. Script 4.1 shows part of the script generated by the database. The script 4.1 shows the settings for one scenario. This part of the script is followed by similar lines with different values if multiple scenarios are simulated.

```
1  ScenarioScript:FaultLocation= 2
2  ;ScenarioScript:FaultResistance= 1.2! in ohm
3  ;ScenarioScript:GridStrength= 1     ! 1 = min values 0 = max values
4  ;ScenarioScript:GeneratedPower= 70  ! Percentage of power generated by the WTs
5  ;ScenarioScript:FaultType= 3        ! 3= short circuit
6  ;ScenarioScript:InvolvedLines= 2    ! 2= L-L fault
7  ;ScenarioScript:ID= 50165           ! Scenario ID
8  ;ScenarioScript:OnTranTap= 12       ! Tap setting of the onshore transformer
9  ;ScenarioScript:OffTranTap= 9       ! Tap setting of the off-shore transformer
10 ;ScenarioScript:33ReacOff= 1        ! 1= 33kV reactor is disconnected
11 ;ScenarioScript:33CapOff= 1         ! 1= 33 kV capacitor is disconnected
12 ;ScenarioScript:220ReacTap= 40      ! Tap position of the On-shore reactor
13 ;ScenarioScript:WTVarA1= -0.26      ! reactive power setting of the WTs at bus A1
14 ;ScenarioScript:WTVarA2= -0.45
15 ;ScenarioScript:WTVarB1= -0.45
16 ;ScenarioScript:WTVarB2= -0.26
17 ;ScenarioScript.Execute();          ! start execution of the interpreter script
```

Script 4.1: Script generated by the database to be used in DigSilent Powerfactory.

Script 4.1 cannot set the settings directly. Therefore, an interpreter script is made which uses the settings from script 4.1 and sets the values. A small part of this interpreter script is shown in script 4.2. This part sets the active and reactive power of each wind turbine string.

```
!!Set Power!!
  s_tmp=GetCalcRelevantObjects('*.ElmAsm');      ! Find all generators in system

  for(o_tmp=s_tmp.First();o_tmp;o_tmp=s_tmp.Next()){ ! Loop around all generators
    if (GeneratedPower>9){                        ! Check if the generated
                                                   power is larger than
                                                   9 because the generator cannot work
                                                   at lower power levels
      PowerWT=GeneratedPower*8/100;               ! denormalize percentage to power

      o_tmp:pgini=PowerWT;                        ! Set power setting
      i_tmp=strcmp(o_tmp:chr_name,'A1');          ! check if the generator is connected to
          bus A1
      if (i_tmp=0){
         o_tmp:qgini=WTVarA1;                     ! Set the reactive power setting
      }
      i_tmp=strcmp(o_tmp:chr_name,'B1');
      if (i_tmp=0){
         o_tmp:qgini=WTVarB1;
      }
      i_tmp=strcmp(o_tmp:chr_name,'A2');
      if (i_tmp=0){
         o_tmp:qgini=WTVarA2;
      }
      i_tmp=strcmp(o_tmp:chr_name,'B2');
      if (i_tmp=0){
         o_tmp:qgini=WTVarB1;
      }

    }
    ! Set other generators to "out of service".
    else{
    o_tmp:outserv=1;
    printf('Undifined Generator');

    }
}
```

Script 4.2: Part of the script that interpenetrates script 4.1.

4.2.2 Output of the Simulation

After every scenario simulation two comtrade files and simulation logs are generated. One simple comtrade file with nine voltage signals and nine current signals; three voltage and current phases for each of the three protection relays (RD1, RD2 and RD3). Another comtrade file with the same signals plus signals with primary voltages, primary currents, crowbar activation and power values at multiple locations in the grid.

The simulation log outputs the powers at the multiple locations in the grid just before the fault is initiated.

These files are numbered with a unique code (Scenario ID). With this code the input data can be found in the database.

4.3 Test

The test is the part of the project where a real protection relay is exposed to the signals generated in the simulation. The response of the protection relay is recorded and saved. This recording can be used for analysis.

4.3.1 Protection Relay Settings

Protection relay settings for the real grid are given. Some of these settings are adjusted to match with the simulated grid. In the real grid multiple protection functions are combined in one protection relay. However, in this test only the distance protection function is programmed in the protection relay. Other functions are therefore disabled in the test.

In the simulation the neutral point of the CT is connected at the side of protected line, equal to figure 2.1. This is conforming to the Siemens standard. However, in the real grid the neutral point is at the busbar side. This is compensated in a protection relay setting.

4.3.2 Test Setup

Table 4.2 gives a list of devices used in the test setup. This list includes the software which is directly involved during the test.

Table 4.2: Devices and software used in the test setup.

Name	Manufacturer & Model	Type/Version
PC	HP	Probook 650 G2
CMC control software	Omicron Advanced Transplay	V3.20
CMC	Omicron	CMC-256 plus
Protection Relay	Siemens Siprotec 5	7SA87-P1A31392
Protection Relay program tool	Siemens DIGSI	V7.50

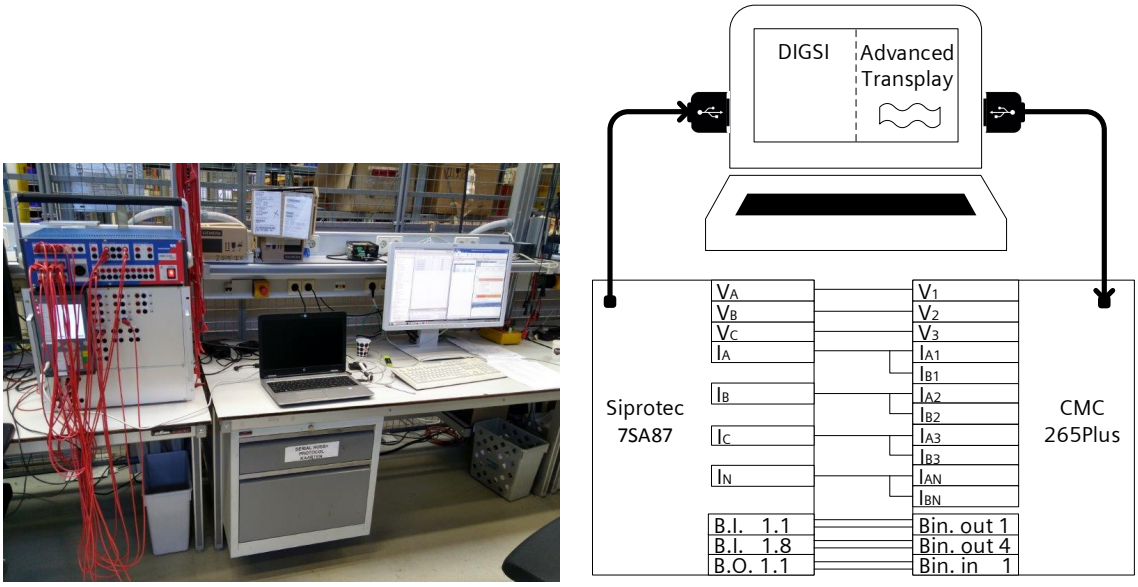

(a) (b)

Figure 4.1: Test setup; photo (4.1a) and diagram (4.1b).

In figure 4.1 a picture and a diagram are shown of the test setup. The PC is connected to the CMC with an USB cable. Multiple cables connect the CMC to the protection relay. Table 4.3 lists these connections.

Note that the current outputs I_{AX} and current outputs I_{BX} on the CMC are connected in parallel. This is done to increase the maximum current generated by the CMC. In some scenarios does the simulation result in a high peak current. To test these simulation a high output current of the CMC is needed. In a parallel configuration can the CMC deliver 25 ampere per current output including I_N.

Table 4.3: Cable connections between the CMC and the protection relay.

Signal type	Designation CMC	Designation Protection Relay	Description
Voltages	$V1, V2, V3$	VA, VB, VC	Secondary Line to Ground (L-G) voltages generated by the CMC.
Currents	$IA1//IB1$, $IA2//IB2$, $IA3//IB3$, $IAN//IBN$	IA, IB, IC, IN	Secondary Line to Ground currents generated by the CMC.
Binary	Bin. out 1	BI 1.1	CMC can feedback to the protection relay that the CB is closed. This function is not used during this test.
Binary	Bin. out 4	BI 1.8	Is only 1 when the files are synthesized.
Binary	Bin. in 1	BO 1.1	Trip signal.

CMC current output $IA1$ is connected in parallel with current output $IA2$ (designated as $IA1//IB1$). Signal "Bin. out 4" from the CMC becomes '1' when the comrade file is played. A setting is made in the protection relay that if BO 1.8 becomes '1' a record will start.

4.3.3 Procedure

To avoid biases all the tests are carried out without looking at the results in between. Around six hours are needed to carry out all the 530 tests for the three protection relays. Prior to the test a list is made with three rows. The first row contains the scenario ID. The second and third rows will be filled during the test. After each test the cell of the second row is filled with the record number generated by the protection relay. The third row will be filled with the time of testing as a check. The procedure to test one scenario is as follows:

1. Load the comrade file with the scenario ID found on the list into advanced transplay.
2. Check if the voltage and current signals will not exceed their maximums.
3. Play the the comtrade file in the CMC.
4. Wait until the CMC is finished synthesizing.
5. Load the records from the protection relay in DIGSI.
6. Write down the last record ID and time on the list.
7. Download the records files, record log files and operational log files to the PC.

When all the tests are done the list is added to the database. For every scenario can easily found back if and when a test is carried out and where to find the data. The next step is to analyze the data.

Chapter 5

Analysis

This chapter will describe the analysis of the results from the test. First the method of analysis is described. After that a brief overview is given of unexpected results with a clear cause. For three groups of unexpected results a detailed analysis is given.

5.1 Protection Relay Response

For each scenario an expectation is made if the relay will trip or not. Figure 3.1 shows for each zone which part of the grid it covers. A protection relay must give a trip signal for each fault that occurs into one of their zones which exceeds the operate delay. The protection relay is not allowed to give a trip signal if the fault occurs outside all its zones. For every zone in each relay for every tested scenario is defined if the fault is in the zone or not in the zone. Since all faults are simulated for one second the expectation is that each relay gives a trip signal if the fault is in the zone.

This expectation is compared to the results from the test. Every expectation that does not match the result from the test is an unexpected result. Multiple scenarios can have the same reason for an unexpected result. These unexpected results are grouped, and each group is analyzed to give a general cause.

5.1.1 Analysis Tool

There are software tools available to analyze fault records in the comtrade format such as Sigra. Sigra is a software tool which displays the signals. It can also do calculations such as impedance calculations. Plots show the signals over time. A large part of the analyzes is done using Sigra. However, during this project was found that Sigra did not fulfill all requirements. One of the downsides from Sigra is that the plots were sometimes very chaotic and not flexible in area of view. It is hard to analyze signals which are chaotic because of the the lag of options of filtering in time and frequency. Another disadvantage is that it takes a lot of time to analyze many comrade files because there is a high number of actions needed to open a cretin plot.

Therefore, an analyses tool is made in Matlab. Scripts from the mathworks website are combined with an own code. This tool is not as user friendly as Sigra but the calculations are all open and each step can be followed. These calculations are based on the Siprotec manual [12] and the results are checked with Sigra. Results are in numerical matrices, so these can be evaluated combined as desired. Another positive effect of writing this program is that it gives better insight of the signal processing of the protection relay.

The filter used in the Matlab script has a lower cut-off frequency than in Sigra. This makes that the plots look more clear, but the transient part is less accurate and a bigger gain is needed. The steady state values are equal. The filter used in the Matlab tool is a low pass filter with a -3 dB point at 100 Hz. A type 2 Chebyshev filter is used with two unique poles and three unique zeros. In some plots is this the filter not used. In a (semi-) stable time range is no filter needed.

5.2 Results

The groups of unexpected results are given in this subchapter. A brief explanation is given for each group. In table 5.1 the properties of the scenarios are given which leads to unexpected results. The used values in the next part are primary values unless noted otherwise.

Table 5.1: Parameters of the scenario for the unexpected results groups.

Unexpected Result group	Relay (RDx)	Fault Loop	Fault Location	Ex. grid strength	Generated Power (%)	Fault Resistance (Ω)	Expectation	Result
1	2	L-L-L	F2	Min & Max	10, 70, 100	0	No Trip	Trip
2	2	L-L-G	F2	Min & Max	0 , 10	1.7	Trip	No Trip
3	1, 2 & 3	ALL	F5	Min & Max	0, 10, 70 & 100	0	Trip	No Trip
4	1	L-G	F4	Min & Max	0, 10, 70 & 100	0	Trip	No Trip
5	2, 3	L-L-L	F2	Min & Max	10, 70 & 100	1.7		
6	3	L-L-G	F1	Min	10	2.25	No Trip	Trip

A simplified overview is of the grid is given in 5.1. This overview includes the fault locations.

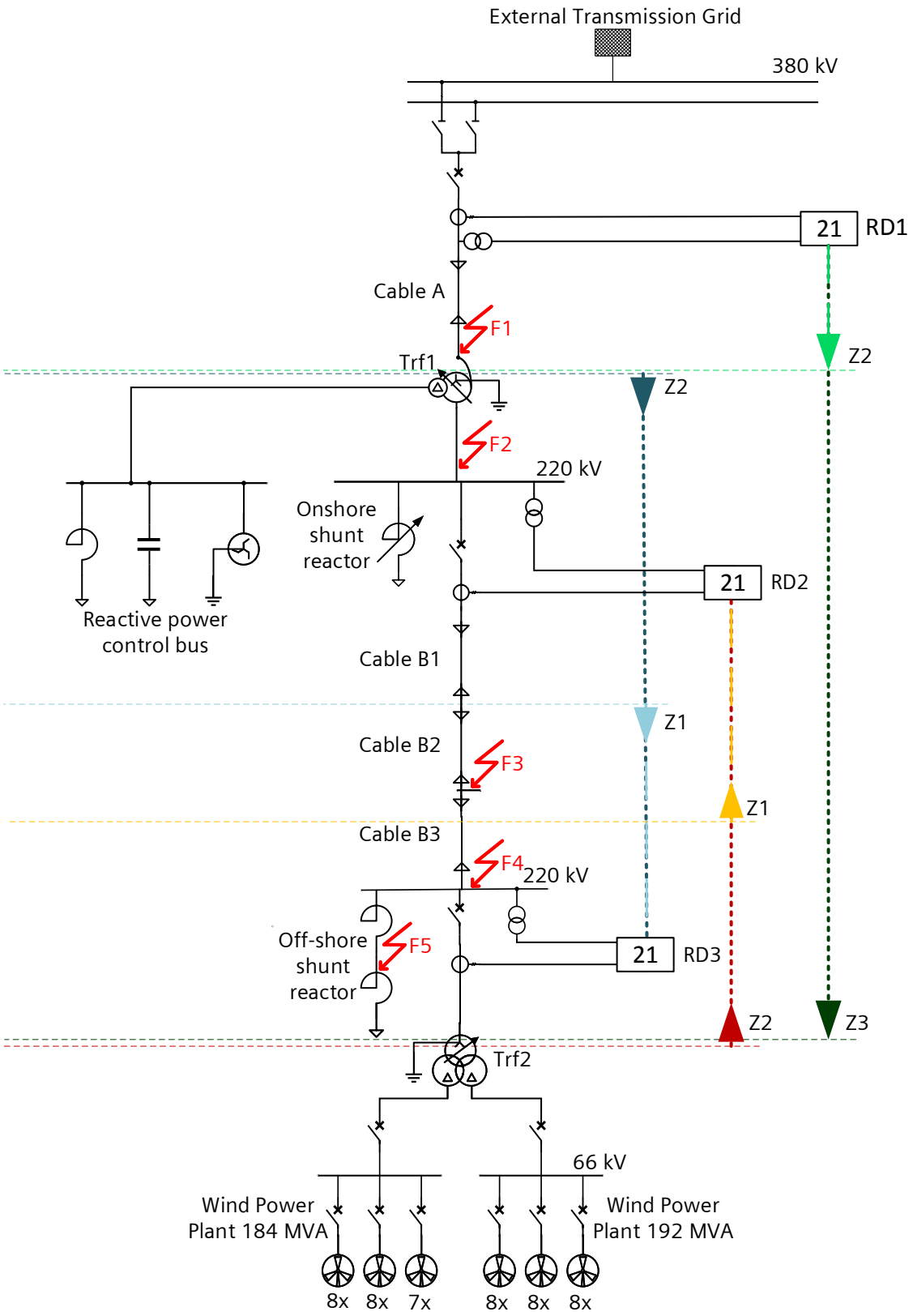

Figure 5.1: Simplified overview of the wind farm grid as modeled including fault locations.

5.2.1 Unexpected results with a clear cause

The results given in this section have a clear cause. These results are briefly discussed.

Unexpected result 1: Zero voltage

The WTs are generating current which does all flow through the fault. The measured voltage during the fault is reaching zero because the protection relay is close to the bolted fault. The direction cannot be determined correctly because of the low voltage. When the fault occurs for 0.75 seconds the protection relay gives a pickup signal and trip signal follows. This phenomenon is seen in multiple scenarios all with a three-phase fault at location F2.

Unexpected result 2: Impedance in a zone without trip

Protection relay RD2 should not trip, and it does not trip. However, in the impedance plot of figure 5.2 can be seen that the $\underline{Z}_{B-G}$ impedance loop is in the zone. $\underline{Z}_{C-G}$ crosses the zone.

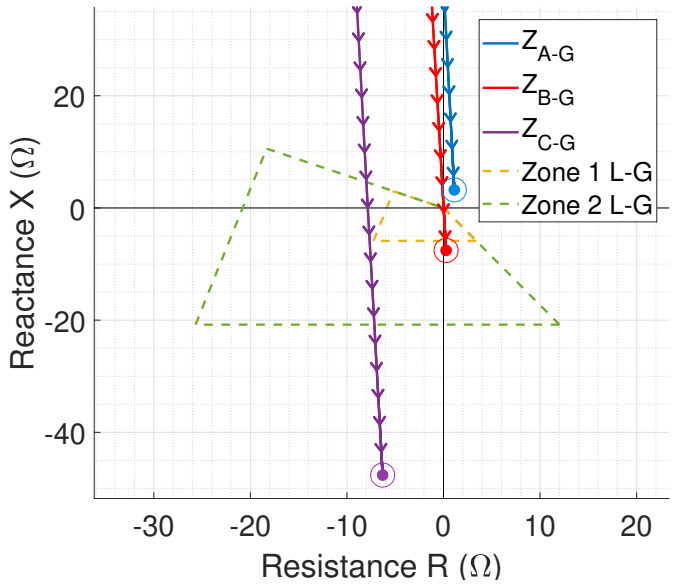

Figure 5.2: Impedance plot of a scenario with an unexpected result.

The result of this situation is as expected. However, a fault is initiated at the forward direction and the zone is set to the backward direction. It can be seen in figure 5.2 that the L-G impedance is represented inside the second zone. The protection relay reacts correctly by not giving a trip signal. The protection relay does detect that the fault type is a two phase to ground with fault impedance. Four tested results show this phenomenon, all with a L-L-G fault at location F2.

Unexpected result 3: High impedance due to current drop.

The measured current drops. This causes the impedance to increase. A low current means that an impedance is not detected. These scenarios have in common that the power generation of the WTs is either 0 % or 10 %. The WTs cannot deliver the fault power. The WTs

shut themselves off and the current decreases under the minimum phase current threshold. Under this threshold the protection relay will not pick-up. There are many scenarios where this phenomenon occurs all at protection relay RD3.

Unexpected result 4: Impedance appears in the zone.

Figure 5.3a shows the impedance plot from one of the scenarios as received from the protection relay. $\underline{Z}_{A-G}$ is visible in this plot inside zone 2. It would be expected that the protection relay will give a trip signal. However, no trip signal is received.

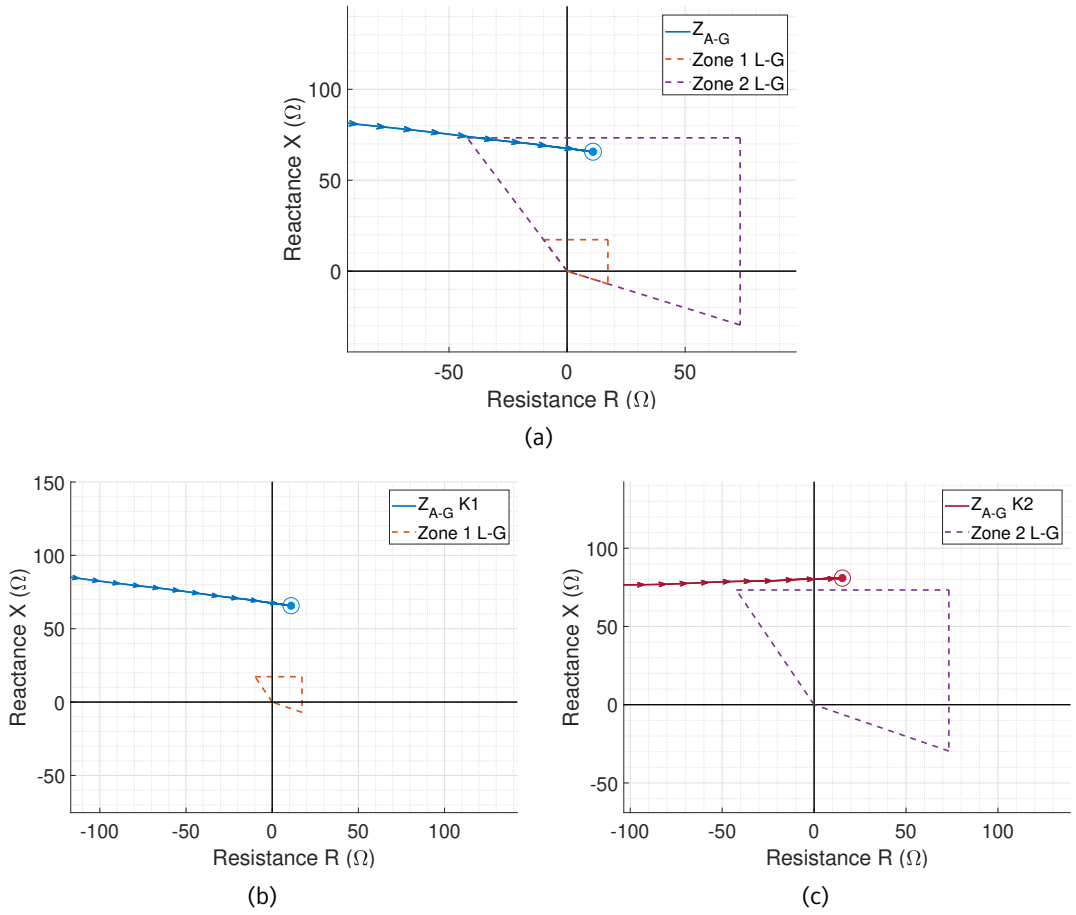

Figure 5.3: Impedance plot L-G fault at F4 measured at RD1.

The RCF is needed to calculate the L-G impedance. This parameter is set in the protection relay. In RD1 a different compensation factor is set for the two zones. This discrimination is made because only the second zone is graded through transformer 1 (Trf 1). The ratio between the ground impedance and line impedance is very different for the two zones.

The L-G impedances depend on this RCF. Therefore, one fault loop has multiple calculated trajectories. Figure 5.3b shows the trajectory for $\underline{Z}_{A-G}$ for K1 with the RCF of zone 1. Figure 5.3c shows the trajectory for $\underline{Z}_{A-G}$ for K2 with the RCF of zone 2. The protection relay gives only a pickup if $\underline{Z}_{A-G}$ for K2 is in zone 2 or if $\underline{Z}_{A-G}$ for K1 is in zone 1.

It can be confusing that Sigra only shows the impedance calculated with the RCF corresponding with zone 1. The .rio file with the protection relay settings does not contain a

second RCF. Therefore, the analysis tool can not know that the zones have different RCFs.

An improvement could be that both RCFs are included in the .rio file. An analysis tool could then include two graphs. One graph for each zone and corresponding impedance trajectories.

5.3 Unexpected Results Explained in Detail

In this subchapter three unexpected results are discussed in detail. These are other scenarios then discussed in subchapter 5.2. The unexpected results listed below have a greater impact on the use of the protection relay and took much more effort to analyze.

5.3.1 Unexpected result 5: Changing Impedance and Voltage Angle

There is combination off two effects in this situation. These two effects are: a radical change of voltage angle after the fault is initiated and a changing fault impedance.

Scenario description

A 3-phase fault is initiated at the onshore 220 kV bus (fault location F2). The fault resistance is 1.7 Ω. The phenomenon occurs at minimum and maximum grid strength The WT generation is 10 % 70% and 100 %. Both protection relays RD2 and RD3 do not react as expected. RD1 responds as expected.

Grid behavior

Two effects in the grid play a major role. The first is the control of the WTs. The WTs have a set-point to deliver a certain active and reactive power. The WT controller tries to keep this power factor.

Seven aggregated WTs activate their crowbar just after the moment that the fault is initiated at 506 ms. The reason is that the rotor current reaches its maximum value. The crowbars are deactivated at 550 ms.

This control of active and reactive power during the fault can be seen in the impedance plots (figure 5.4). From the results can be calculated that the impedance does change with 34 Ω per second after the transient. It can be seen in the impedance plot that the impedance stays in zone two.

Like any other fault the fault circuit differs from the normal circuit, the magnitude and angle immediately change after the fault is introduced. This change in reactance causes the voltage angle measured at the location of the protection relay to rotate. In the simulated scenario the voltage angle does rotate more than 60°.

Protection relay behavior

Figure 5.4 shows the impedance plots of RD2 and RD3. The letters A,B,C,Z and Y denote important time points. These points are listed in table 5.2. The fault is initiated at 500 ms.

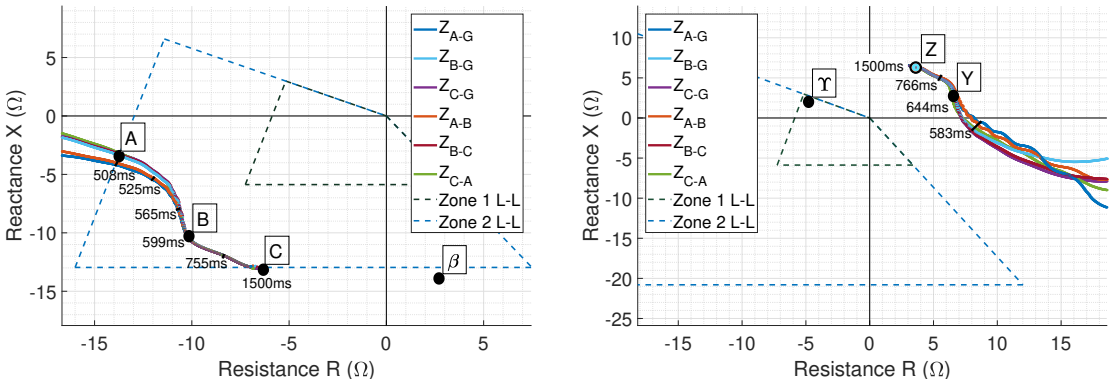

(a) (b)

Figure 5.4: Impedance plot of RD3 (5.4a) and RD2 (5.4b).

Table 5.2: Important time points during these scenarios.

Letter in figure 5.4	Time (ms)	Description
A	508	The impedance enters the zone. A pickup is received for the $L_A - G$, $L_B - G$ and $L_C - G$ fault loop.
B	599	The pickup signal is turned off.
C	1500	End of the simulated fault.
Y	644	A pick-up signal is received.
Y	674	A trip signal is received in for zone 1.
Z	1500	End of the simulated fault

In RD3 the fault impedance is inside the second zone. A trip is expected after the operate delay of 230 ms. The relay gives a pickup signal when the fault occurs. However, this pickup signal will be turned off after 113 ms. No trip is received. The fault impedance changes but it stays inside the second zone.

RD2 gives a trip signal when no trip is expected. The impedance plot from Figure 5.4b shows that the three-phase fault impedance is at the opposite site of the zones. However, a trip signal is given by the protection relay. A trip signal is unexpected because the impedance is not inside the zone.

Finding the cause

At 600 ms the trip signal tuns off. This is five cycles after the fault is initiated. Most of the transient effects are vanished. The fault is balanced it can be assumed that the voltages and currents only have a positive-sequence component.

Extra tests are done to find the cause of this result. In one of these tests the comtrade file is manipulated by repeating one cycle during the fault for 12 times. This keeps the impedance stable for 240 ms. The signals are fed into RD3. A repetition of one cycle for 240 ms results in a trip. This shows that the unexpected behavior of not tripping has something to do with the changing impedance.

Hand calculation

A hand calculation is carried out to give a deeper insight in this scenario. Another main purpose of the hand calculation is to check if the voltage jump is reasonable. Appendix 7 shows an full explanation of the hand calculation.

In this scenario a three-phase fault is initiated. The grid is assumed to be balanced. Therefore, only the positive-sequence component is present. This makes the calculation easier. A simplified positive sequence circuit is derived to calculate the normal and fault condition currents and voltages.

Figure 5.5 shows the equivalent positive sequence circuit which is used in the hand calculation.

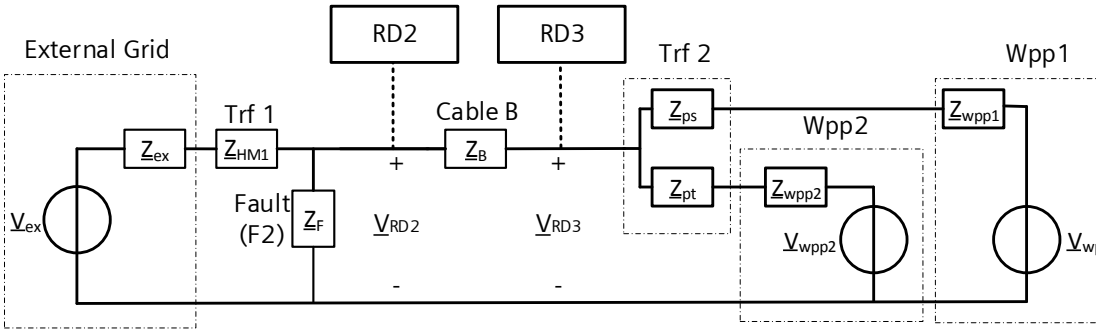

Figure 5.5: Equivalent positive sequence circuit including a thee phase fault at location F2.

Voltages and currents are derived for the locations where protection relays RD2 and RD3 measure. The calculated voltages for RD2 and RD3 during the fault are respectively 11.7 kV$\underline{/-74^\circ}$ and 17.6 kV $\underline{/-9^\circ}$. These voltages in normal operation are respectively 128 kV $\underline{/8^\circ}$ and 131 kV $\underline{/11^\circ}$. The voltage angle jump from before and during the fault condition can now be calculated. The differences in voltage angles are 20° for RD3 and 82° for RD2.

A 60° phase jump in the simulation is high but reasonable. The voltages shown above do reveal that cable B is a major contributor of the high phase jump. It can be seen that the phase difference between the two sides of the cable is only 3° in normal condition. However, in fault condition the difference is 39°. This is due to the high resistance/reactance ratio of 0.25 of the loop impedance. This ratio will further increase when the purely resistive fault resistance is included.

In normal condition the current through the cable is low in comparison to the fault condition. Therefore the voltage angle change difference over the cable is low. In fault condition is the voltage drop over the cable much higher. A high resistance/reactance ratio compared to the rest of the system does lead to a high voltage angle difference.

Wind turbine control

The model is adjusted to investigate the influence of the wind turbine control on this scenario. A special simulation has been ran where the control of the wind turbine is interrupted just before the fault is initiated. This is done to initiate the fault in an equal condition. During the fault the control does not have an influence.

In figure 5.6 can be seen that the fault impedance is stable at $-4.7 + 6.3j\ \Omega$. This is comparable with the short circuit calculation and the result of the hand calculation.

The the test response of this scenario was a trip signal. This is the expected result and shows that the unexpected behavior is correlated with the wind turbine control.

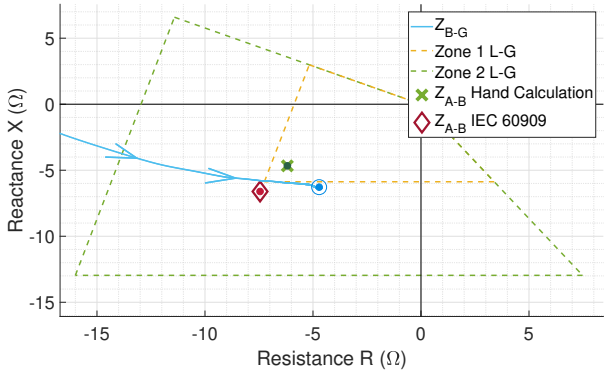

Figure 5.6: Impedance plot of RD3, result for the hand calculation and IEC 60909 and the EMT simulation result where the wind turbine control is tuned off .

Testing on another type of protection relay

These scenarios are also tested on a older generation of protection relay. A Siemens Siprotec 4 type 7SA631 protection relay is used for this test. The 7SA631 responds exactly as expected. It is surprising that the older type of distance protection reacts better to this fault as the newer type.

Theory

A theory is made to explain the behavior described in this section. First will be focused on the behavior of RD3.

The protection relay behaves as expected when the fault is initiated. A pick-up signal is received at the moment that the impedance enters the zone. This pick-up signal stays active for 113 ms.

The theory is that the protection relay switches to another calculation method at the moment that the pick-up falls off. The algorithm desired to change the calculation method because of the moving impedance. In this calculation method the pre-fault voltage is used. The calculate impedance rotates outside the zone. This happens because the pre-fault voltage is used which has another angle. The result of the new calculation sets the impedance outside the zone. If the protection relay concludes that the impedance is outside the zone does it retract the pick-up signal.

Essentially the same happens with RD2. However, the second calculation method sets the impedance inside the zone instead of the opposite side. The calculated loop impedance with the pre-fault voltaged is designated in figure 5.4 with "Υ" for RD2 and "β" for RD3.

Switching to another calculation method is normal for a protection relay. Multiple calculation methods are used depending on the time and depth of impedance into a zone. Hermann [14] gives a detailed description about this process in his book. The test where part of the fault is repeated shows that this switching of calculation method is induced by the moving impedance.

This theory could not be confirmed because more information is needed on the internal working of the protection relay. The development team has to be contacted to get the information to confirm this theory.

Possible solutions

In this paragraph is a solution given is if the above mentioned theory is true.

In this project distance protection with the classic method is used. However, the RMD method can handle this scenario better because it uses a flat decision tree. Therefore, the L-G loop impedance is simultaneously calculated with the pre-fault voltage and the present voltage with RMD. An incorrect decision in the decision tree is not fatal in RMD.

For one of the scenarios gave RD3 a trip signal using RMD while no trip signal was given using the classic method. However, other scenarios still gave an unexpected result with RMD.

5.3.2 Unexpected result 6: Arc-resistance reduces calculated impedance

In these scenarios no trip is expected because F1 is calculated outside the zone of protection relay RD3. However, the impedance is calculated inside zone 2. Therefore, the protection relay gives a trip signal.

Scenario description

This phenomenon does only take place with RD3. This is the only protection relay which protects in the direction of the external grid. Every scenario has a L-L-G fault at location F1 and a fault resistance of 2.25 Ω. The generated power from the WTs is 10%. The unexpected result does only occur at minimum grid strength. However, at maximum grid strength has the L-G loop impedance also an incorrect value.

Grid behavior

A simplified circuit of the grid with the fault is shown in figure 5.7. Most of the current flows through the fault resistance to ground.

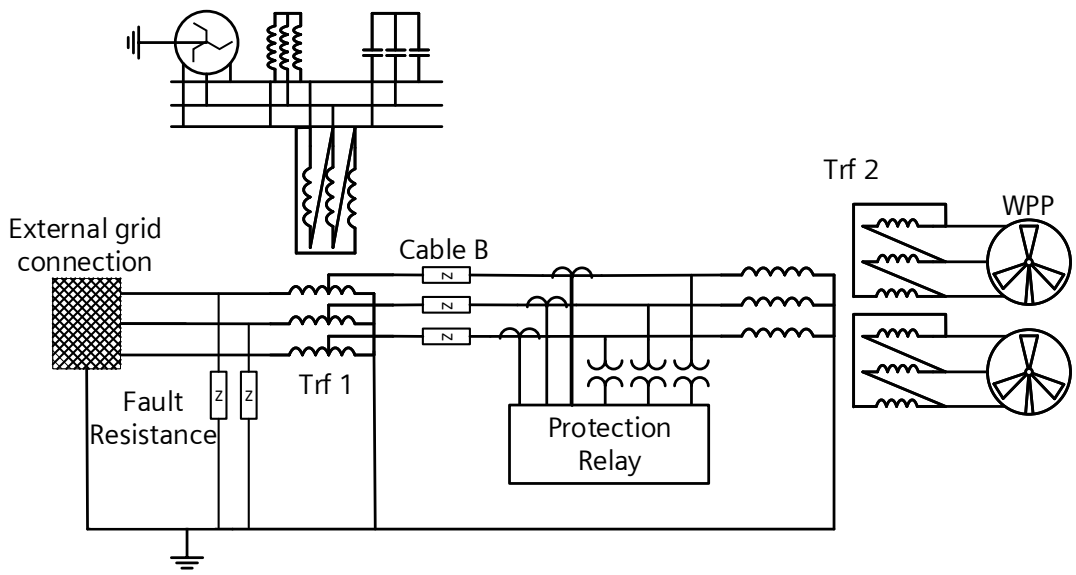

Figure 5.7: Simplified representation of the grid with a L-L-G fault at location F1.

Protection relay behavior

The fault at location F1 is outside the area protected by RD3. Nevertheless, the impedance is calculated inside zone 2. Figure 5.8 shows the impedance plot of this scenario with multiple calculation methods.

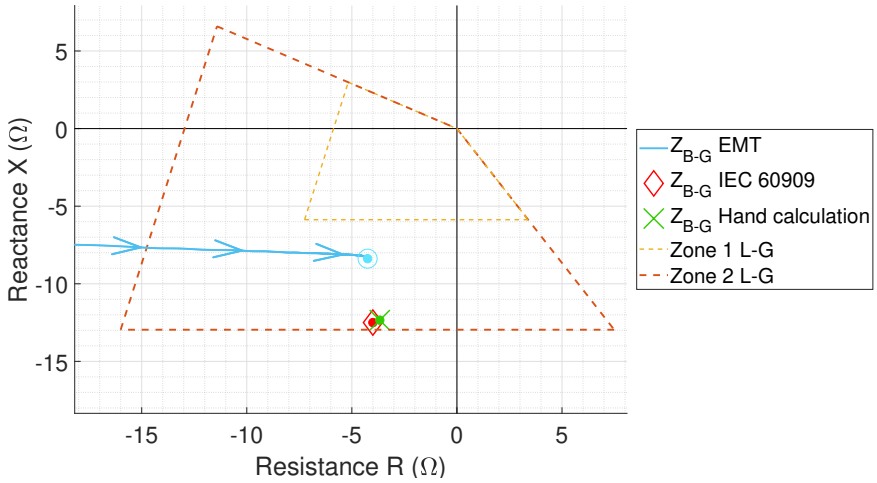

Figure 5.8: Impedance plot the L-G fault loop impedance measured with RD3.

For this scenario no test was needed. The extraction from the simulation could be imported directly into the analysis tool to see the impedance plot. Therefore, this unexpected result is not caused by the protection relay.

Extra Calculation

Two types of calculations are carried out according to the IEC 60909 to analyze this scenario. A short circuit simulation in DigSilent PowerFactory and a hand calculation.

Short circuit simulation

A short circuit calculation in DigSilent PowerFactory calculates the steady state voltages and currents. Additionally, it does calculate the impedance which is also calculated by the protection relay. This is a different type of simulation as the EMT simulation used in the test. The same model is used where some parameters are different. Figure 5.8 shows that the calculated impedance is different for the two calculation methods. However, a faulted L-G loop impedance also appears in zone 2. The smallest calculated L-G impedance for this scenario is -4.0-12.5*j Ω.

Hand calculation

To give a deep insight in what happens in the grid a calculation is carried out by hand. The sequence networks method is used [29]. The equivalent sequential sequence network to consider this scenario can be found in figure 5.9.

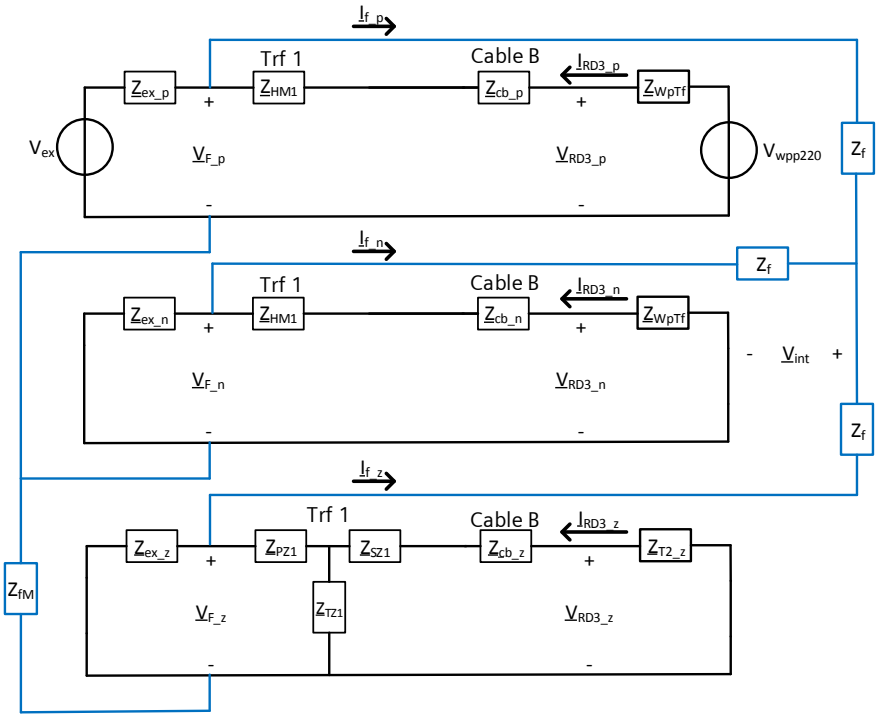

Figure 5.9: Sequential components network of a L-L-G fault at fault location F1

The values are converted back to the line phasors at the location of RD3 to determine the impedance. Only the dominant equipment is considered. For cables only the series impedance is considered. Shunt reactors have been left out to simplify the calculation. The hand calculation is organized in a Matlab script. Intermediate values are checked with the short circuit simulation. The hand calculation and short circuit simulation differ with 2%. This is mainly caused by the simplification of the grid. The calculated $L_B - G$ impedance is -4.3-16.7j Ω.

Finding the cause

It is remarkable that the measured impedance decreases if the fault resistance gets larger. A fault impedance of 4 Ω puts the calculated impedance in zone 1. A fault impedance of 5 Ω sets the calculated impedance outside the zone. Figure 5.10 gives the impedances measured by RD3 for a range of fault impedances.

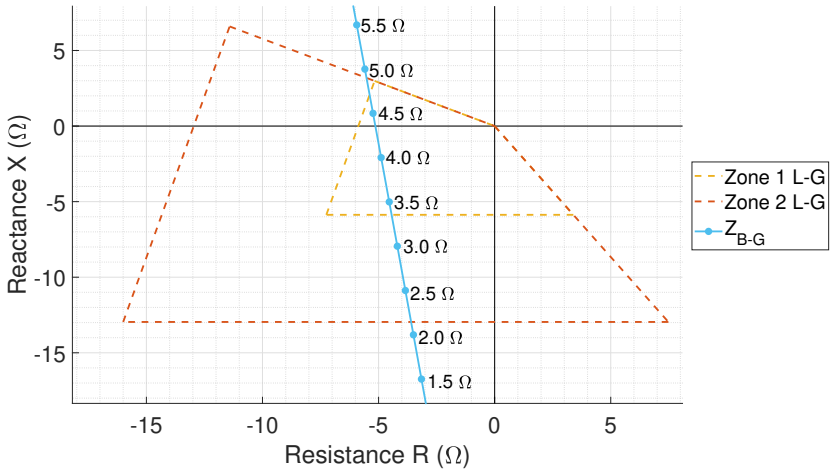

Figure 5.10: Plot of the impedance measured by RD3 for different fault impedances

There must be a deviation between the real and calculated impedance. The origin of equations 2.4 and 2.5 are analysed to find this deviation. In the book of Ziegler [13] can be found that these equations are derived from kirchhoff's voltage law considering the fault loop. Figure 5.11a gives the assumed fault loop for the impedance calculation.

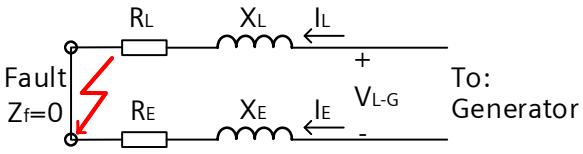

(a)

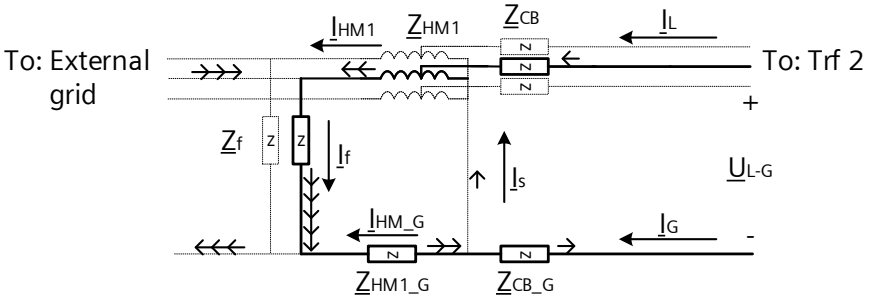

(b)

Figure 5.11: Typical fault loop which is used as a basis for the impedance calculation (5.11a) and the real fault loop for this scenario (5.11b). The solid line is the fault loop, the dotted line is part of the system that influence the fault loop.

With Kirchhoff's voltage law the following equation can be found:

$$\underline{U}_{L-G} = \underline{U}_{nl} = \underline{I}_L \cdot R_L + j \cdot \underline{I}_L \cdot X_L - \underline{I}_E \cdot \frac{R_E}{R_L} \cdot R_L - j \cdot \underline{I}_E \cdot \frac{X_E}{X_L} \cdot X_L \tag{5.1}$$

Where $\frac{R_E}{R_L} = k_R$ and $\frac{X_E}{X_L} = k_X$ are the complex parts of RCF. Equation 5.1 can be rewritten to determine R_L and X_L. Figure 5.11b represents the real fault loop. The short arrows show the currents in the system which flow trough line B. It does also show how these current continue their path. Currents which flow through line A and C are not represented in this figure.

Some differences are noticeable if the theoretical fault loop is compared to the real fault loop. These differences are:

- Voltage drop over the fault impedance is not considered.
- The fault loop contains a transformer which does change the ratio between the line and ground impedance.
- The grounded star point in the autotransformer creates an extra branch in the return path.

The highest influence is caused by the first point. In appendix 4 the effect of these three differences is calculated on the loop impedance. The following sections give more information about these items.

Voltage drop over fault impedance

The voltage drop over the fault impedance is not included in equation 5.1. This is the main cause of the unexpected behavior of this scenario. The fault is close to the external grid. Therefore, the current contribution from the grid is relatively high and causes a high voltage drop over the fault impedance. The relay cannot detect this high current since it is located at the WPP side fault.

In appendix 3 the voltage over the fault impedance is calculated. The fault voltage in the $L_B - G$ loop has a magnitude of 15 kV. This is significant since the voltage measured by RD3 has a magnitude of 52 kV.

The phenomenon that an increase of fault impedance decreases the measured impedance is explained by the significant voltage drop over the fault impedance. Most of the current through the fault impedance is supplied by the external grid. A higher fault impedance means a higher voltage drop over the fault impedance. This has as effect that the impedance calculation differs more from the real impedance.

Change of ratio between the line and ground impedance

To compensate between the difference in impedance of the line and the ground path, the RCF is set in the protection relay. This ratio is different in a transformer. If the transformer was considered it decreases the total RCF. It is not advisable to change the protection relay setting since it would not be valid for faults within the protected area. The alternative RCF if the transformer was included is: $k_{alt} = 2.92 + 0.033\,j$

The transformer changes the return path

Figure 5.9 shows that the zero-sequence circuit has a branch in the transformer. This has as effect that a part of the zero-sequence current flows through $\underline{Z}_{L\_z}$. This prevents it to be

measured by the relay as $\underline{I}_G$ $(= 3 \cdot \underline{I}_{RD3\_z})$. The calculated loop impedance, if compensated for this effect, of line B is calculated at: $\underline{Z}_{L_B-G} = 3.2 + 8.0j\ \Omega$. It can be seen that this impedance is smaller and deeper in zone 2. This means that if the star point current increases the calculated impedance increases.

Compensation of all distorting factors

In appendix 4 can be found that equation 5.1 can be rewritten to split U_{L-G} into three parts:

$$\overbrace{\underline{U}_{L-G} = \underline{U}_{nl}}^{\text{Loop voltage assumed by the protection relay}} + \overbrace{\underline{U}_s}^{\text{Voltage caused by the grounded star point}} + \overbrace{\underline{U}_f}^{\text{Fault voltage}} \tag{5.2}$$

A more accurate loop impedance can be calculated if U_s, U_f and the alternative RCF are considered in equations 2.4 and 2.5. The impedance can be calculated using:

$$R_{L-G} = \frac{Real(\underline{U}_L - \underline{U}_s - \underline{U}_f) \cdot Real(\underline{I}_L - k_{x\_alt} \cdot \underline{I}_E) + Imag(\underline{U}_L - \underline{U}_s - \underline{U}_f) \cdot Imag(\underline{I}_L - k_{x\_alt} \cdot \underline{I}_E)}{Real(\underline{I}_L - k_{r\_alt} \cdot \underline{I}_G) \cdot Real(\underline{I}_L - k_{x\_alt} \cdot \underline{I}_G) + Imag(\underline{I}_L - k_{r\_alt} \cdot \underline{I}_G) \cdot Imag(\underline{I}_L - k_{x\_alt} \cdot \underline{I}_G)} \tag{5.3}$$

$$X_{L-G} = \frac{Imag(\underline{U}_L - \underline{U}_s - \underline{U}_f) \cdot Real(\underline{I}_L - k_{r\_alt} \cdot \underline{I}_G) + Real(\underline{U}_L - \underline{U}_s - \underline{U}_f) \cdot Imag(\underline{I}_L - k_{r\_alt} \cdot \underline{I}_G)}{Real(\underline{I}_L - k_{r\_alt} \cdot \underline{I}_G) \cdot Real(\underline{I}_L - k_{x\_alt} \cdot \underline{I}_G) + Imag(\underline{I}_L - k_{r\_alt} \cdot \underline{I}_G) \cdot Imag(\underline{I}_L - k_{x\_alt} \cdot \underline{I}_G)} \tag{5.4}$$

This evaluated gives for line A, B and C a calculated loop impedance of:

$$\underline{Z}_{L_A-G} = -1.8 - 28.3j\ \Omega$$
$$\underline{Z}_{L_B-G} = -1.7 - 24.3j\ \Omega$$
$$\underline{Z}_{L_C-G} = -11 - 163.9j\ \Omega$$

Possible solutions

The RMD method uses another calculation method. It tries to calculate the voltage over the fault resistance using the negative sequence current or zero sequence current. Thus, the RMD method takes the voltage over the resistance into account. This means that the RMD method can estimate the fault loop impedance.

Tests show that the distance relay reacts correctly for this scenario if the RMD method is used.

5.4 Remarks on shunt reactor

None of the protection relays could detect a fault at location F5. The impedance of the off-shore shunt reactor is too high. The change of power factor has no crucial effect on the distance protection. The current reactor is in the zone. However, it could be calculated that this distance protection configuration is not suitable for fault detection at F5. It is expected that only a fault very close to the terminals could have an effect of the distance protection function.

Chapter 6

Discussion

In this project the distance protection of an offshore transmission grid is studied. There has been looked if the protection relays work as desired considering a wide range of situations including multiple infeed levels from the wind power plant.

In this chapter is assessed if the project is approached correctly.

6.1 Challenges in protection

In literature has been found that protection of grids deals with challenges. These challenges are first described in subchapter 2.3. In following paragraphs is reviewed if these challenges do also occur in the test of this project.

Large fault resistance

Some researchers have found that a large fault resistance could lead to not detecting the fault [6]. In this project an approximation is made of the largest fault resistance which is likely to occur. The largest fault resistance simulated is 2.25 Ω. No scenario is found where the fault impedance exceeds the R-reach of the zone. However, in unexpected result 6 does the fault impedance cause a decrease of the calculated L-G loop impedance. In these cases, a trip signal is received while no trip signal was expected.

This phenomenon is described in section 5.3.2. In the calculation of the L-G loop impedance is not accounted for the relatively high voltage drop over the fault resistance. The main contributor of the current through the fault resistance is from the external grid. This is a component that is not measured by the protection relay.

Low energy production

Multiple studies report on unreliable behavior of distance protection if generation is low [6, 15]. Many tests from this project confirm this statement. Unexpected result 3 in subsection 5.2 describes this phenomenon. It is expected that the influence of not tripping a CB at low generation is low in most cases. It is not a problem since the other protection functions and other relays will take over and open the CB. In a renewable energy grid there is a change that a CB does not trip at low generation. It is important that this is considered in the design.

Transients

A study by Li et.al. [15] does carry out similar tests. In this study unintended trip signals are given by protection relays during transients caused by the grid. The design of these tests where very similar to the tests at this project. No equal malfunctions of the protection relay are found in this project.

However, these tests could be compared to unexpected result 5. In this scenario is a L-L-L fault initiated. The measured L-L loop impedance changed during the fault because of the WT controller.

In this situation it is not a transient caused by the grid behavior that is causing the lag of giving a trip signal but a relatively long transient caused by the WT controller operation. The impedance changes which makes it more difficult to calculate the impedance just like the behavior of transient in the study of Li et.al.

Global information is available on the use of multiple calculation methods inside the protection relay. More detailed information is needed from the test and the algorithms of the protection relay to see if the two cases are comparable. It is useful to know on what basis each calculation method is used. It could also help to know what the input values are for each calculation method.

Transformers

For many scenarios transformers are partly responsible for the unexpected result. RD1 and RD3 both are graded through transformer 'Trf 1'. For unexpected results 5 and 6 both a transformer is present between the protection relay and the fault. The ground path impedance differs widely from a situation where only a cable is graded. Therefore, the RCF needs to be adjusted for a zone which crosses a transformer. This is also backed in the book of Ziegler [13].

Crowbar

During the analysis special attention has been paid to the effect of the crowbar circuit. Caution has been taken because a paper by Lina He and Liu [30] warns for the effects of the crowbar circuit on the protection relay. In some simulations the crowbar is activated. However, no scenario has been found where the crowbar circuit causes an unexpected result.

6.2 Grid

How the grid is modeled plays a major role in this project. In this subchapter is reviewed which parts of the grid was worth to model and which was not.

Grid model

The grid layout and protection relay settings for the protection relay are given. This grid layout is derived for a particular WT grid. The disadvantage of using this layout, and protection relay settings, is that it makes the scenarios more specific. This goes against the wish to make the project general.

An advantage of the grid model is that it is based on a real grid. Which shows that the results of this study are valid for a real scenario.

External grid

The external grid itself was a key part of the simulation. There has been differentiated between maximum and minimum grid strength. This differentiation has an effect on one unexpected result. In unexpected result 6 does the grid strength play a role. An unintended trip does only occur at minimum grid strength. Thus, it gave extra information to model two variations of the grid.

Wind turbine model

A type 3 WT model is used in this project. A given template is adjusted for this simulation. A large disadvantage of this model is that it is uncertain in what amount this model differs from a real WT. At the moment of modeling limited data was available of the real WTs. Using data from a real WT manufacturer would be a enrichment of this project. On the other hand, the purpose of this project was to be general and not only applicable for one wind farm. Therefore, this study is useful for future wind farms with a similar wind farm grid.

Transformer saturation

Saturation effects are considered in the models of transformers and reactors. None, of the causes of unexpected results could be traced back saturation effects. This does not mean that it has no influence.

Cable model

Considerable care has been taken into the cable model. Cable B is modeled with a distributed parameter model. A distributed parameter model is marginally more accurate at than other cable models. The effort to implement is low. However, the effort to demonstrate which model was suitable for each cable was high.

Power depended grid settings

There has been chosen not to implement the park controller but to use power depended grid settings. This turned out to be a good alternative because it makes the simulation simpler. Another benefit is that similar scenarios have equal setpoints and tap positions.

6.3 Unexpected results

In the cases with unexpected results the cause of these results can be: an unexpected behavior of the grid, unclarity of the analysis software or an incorrect interpretation by the protection relay.

Extra effort is put into two groups of unexpected results. Theories are formed to explain the reason for these unexpected results. Not all aspects of the theories could be confirmed because more information from manufactures is needed.

In the first group (unexpected result 5) does protection relay RD2 give a trip signal while this is not expected and RD3 does not give a trip signal while a trip is expected. Characteristic for these scenarios is that the impedance does change after the transient.

This change of impedance is caused by the control of the WTs. This in combination with a change of voltage angle has as effect that no trip signal is given.

In the second group (unexpected result 6) a L-L-G impedance is initiated outside the zone. However, the calculated L-G fault loop impedance is calculated inside the zone. Extra calculations show that a higher fault resistance results in a lower impedance measured by the protection relay. This property is counter intuitive since more resistance added to the fault loop should result in a higher measurement.

Calculations show that the external grid produces a fault current through the fault resistance. This creates a voltage over the fault resistance. The protection relay does not account for this voltage in the L-G fault loop.

6.4 Developed tools

During this project two tools are developed to improve the quality and efficiency of the project. The first tool is the database to store data. The second is a comrade analysis tool. In this subchapter reflects if it was useful to develop the tools and if the effort was worth the benefits.

6.4.1 Database

At the beginning of the project there was started with an spreadsheet to store all data. The spreadsheet became too large and deficient. Therefore, there was decided to switch to a database. The database does not only have the function to store data and pointers to data but can also generate a script to control the simulations. The effort was low since it was easy to import the original spreadsheet file into a database. The knowledge was already available to work with a database management system. Making the simulation control script took more effort. However, the alternative would be to set the parameters for each scenario by hand which would be a much greater effort.

Comrade analysis tool

The idea behind the Matlab analysis tool was to completely replace Sigra with a better tool. This turned out differently. The two tools complement each other. Sigra can be used for quickly analyzing a single comrade file with the confidence of getting trustworthy results. In the Matlab tool can each step of calculation be examined in detail. Moreover, the code can be changed to turn off the filter or many files with minimum effort. Figures can be created as desired. It took a high amount of time to develop this tool. However, it gave new possibilities in analyzing.

6.5 Improvements and Further research

This project is a basis with interesting results. However, the project could be expanded with extra grid variations and scenarios.

6.5.1 grid model expansion

In this section extra scenarios are proposed for a follow-up study.

More advanced arc model

A better model could be used for the arc. The arc resistance changes over time.

For example an arc in open air can be affected by wind. Wind can make the arc longer which increases the arc-resistance. It would be interesting to model this increasing arc-resistance over time. Especially, since it has been found in that changing impedance can have an undesired effect on the protection relay in unexpected result 5. In Unexpected result 6 plays the fault resistance a major role. A more advance arc model could give better insight in the situations.

Wind turbine model

In this project only a type 3 WT model is tested. Type 4 WTs are also widely used. Simulating the scenarios with an type 4 WT model can make the project more general. An ancillary is that the response of the two model can be compared. It would be more trustworthy if the wind turbine use parameters derived from measured values.

Fault in transformer

Two protection relays are graded through transformer 'Trf 1'. It would be interesting to model a fault inside this transformer. An extra type of fault could be a turn-to-turn fault in the same winding. This takes extra effort since the transformer needs to be split into two or more parts to keep it representative.

6.5.2 Increase automation

The number of scenarios that could be tested depend on the level of automation. In this project the simulation is automated, but the testing is partly manual. A fully automated test setup increases the number of tests that could be carried out in a reasonable time. For this control of the CMC is needed. Automatically downloading and administering the records would be the next step. It is expected that only a small effort is needed to automatically analyze the records if the trip signal is given.

A fully automated test setup is not only beneficial for research but can also be used as standard procedure for testing protection schemes. This would increase the change of finding an imperfection in a protection scheme. This will mean that the reliability of electricity grids will increase.

6.6 Advice for future protection schemes

Some lessons can be learned from this project for the design of protection schemes.

Transformers

Be very careful with grading through transformers. The ratios line impedance/ground impedance $\frac{X_L}{X_G}$ and $\frac{R_L}{R_G}$ (RCF) are often very different for a cable and a transformer. This makes it difficult to get an accurate impedance measurement with a cable and a transformer in one zone. It is advised to use a dedicated zone for the transformer. This zone needs its own RCF. All decisions need to be backed with a model and logic thinking.

Check data

Check if the data you receive from the protection relay (or other digital equipment) is correct. Check if multiple L-G impedance are visible for each line if multiple RCFs are used. Check if the zones are correct. Check if the measurement setup is correct. If possible, check if the steady state impedances match with the expected value.

Distance protection with the reactance method

In this project the distance protection with the classical method is used. However, the RMD distance protection function can perform better in some scenarios. For example, the scenarios of unexpected result 5 and 6. Moreover, the RMD distance protection function is recommended by the developers of distance protection.

Use multiple protection functions

Every protection function has its down side. The advice is to use multiple protection functions for each area in the grid. A backup protection function can be used if the main protection function fails. Most Siprotec 5 devices have the capability to use multiple protection functions simultaneously. Even better would be to use a redundant setup of protection relays.

Keep it as simple as possible

From the test has become clear the zones protecting one single cable almost always respond as expected. If possible, only protect the cable close to the ITs. Thus, do not grade equipment far from the distance relay.

Chapter 7

Conclusion

In this project faults are simulated in a wind farm grid model. Several scenarios have been simulated with different kind of faults at multiple locations. The secondary values of the CTs and VTs are extracted from the simulation to a file. These files are synthesized to real voltages and currents. These signals are fed into a Siemens Siprotec 5 protection relay. The response of the protection relay is analyzed.

A summary of answers to the research questions are listed. Starting with the sub-questions and ending with the main question.

1. What is a good method to test the response of a protection relay on the dynamic behavior of the grid?

   The best method to analyze the response of the protection relay depends on the available resources. After much deliberation has been chosen to use DigSilent PowerFactory as partly simulation software in combination with the Omicron CMC. It can be concluded that this was a suitable choice for this project. A hardware in a loop setup was not needed since the reaction of the protection relay to the grid is not studied.

2. How does an autotransformer effect the impedance determination in the protection relay?

   Grading through an autotransformer is possible. However, it takes caution in the calculation and fault analysis. If grading to an autotransformer is desired it is advisable to use a dedicated zone for the autotransformer with a dedicated RCF. It is advisable to check the settings with calculations on undesired underreach or overreach.

3. Does the distance protection function of a protection relay handle the dynamic behavior of a WT correctly?

   There are results from the test where it is expected that incorrect behavior of the protection relay is caused by the dynamic behavior of the WTs. The scenarios are rare but realistic.

4. What issues can disturb the function of the distance protection function in the protection relay?

   The challenges that came up in this project are: fault resistance, low energy generation by the WTs, dynamics of the WTs and grading through a transformer.

5. Can a fault in a shunt reactor be detected with the distance protection function of a protection relay?

   In this project several scenarios with a fault are modeled at 50 % of a shunt reactor. None of these faults are detected by the distance protection. Faults closer to the terminals may be detected by the distance protection.

The main question can now be answered.

Does the conventional distance protection relay respond correctly to all faults in a wind farm electrical grid?

No, the tests from this project show that the protection relay does not respond correctly to all scenarios. Tests confirm that the protection relay in 468 of the 530 cases react as expected. The cause of the other 62 cases is not always certain since not all data is available and not all results could be mathematically explained. The theories made in this project point out the following causes: behavior of the simulated grid, incorrect interpretation of the results and the interpretation in the protection relay.

Despite this negative answer distance protection is an effective protection function. Every protection function has its downsides. It is advised that always two types of protection functions are used, one main and one or more backup. Distance protection must carefully be implemented backed with calculations and the correct grid data.

Bibliography

[1] L. Fried, S. Shukla, S. Sawyer, and S. Teske, "Global wind outlook 2016," Clobal Wind Energy Council (GWEC), Tech. Rep., 2016.

[2] M. Schmela, G. Masson, and N. T. Mai, "Global market outlook for solar power 2016-2020," *SolarPower Europe*, 2016.

[3] F. Straver and B. Zuidervaart, "Het nationale klimaatakkoord: nog geen reden voor een feestje," *Trouw krant*, July 2018.

[4] B. Fardanesh and E. F. Richards, "Distribution system protection with decentralized generation introduced into the system," *IEEE transactions on industry applications*, vol. 3, pp. 122–130, 1984.

[5] J. B. Patton and D. Curtice, "Analysis of utility protection problems associated with small wind turbine interconnections," *IEEE Transactions on Power Apparatus and Systems*, vol. 10, pp. 3957–3966, 1982.

[6] S. De Rijcke, C. Moors, P. Souto Pérez, and J. Driesen, "Impact of wind turbines equipped with doubly-fed induction generators on distance relaying," *IEEE PES General Meeting*, 2010.

[7] A. Hooshyar, M. A. Azzouz, and E. F. El-Saadany, "Distance protection of lines connected to induction generator-based wind farms during balanced faults," *IEEE Transactions on Sustainable Energy*, vol. 5, no. 4, pp. 1193–1203, 2014.

[8] E. Harder, B. Lenehan, and S. Goldsborough, "A new high-speed distance-type carrier-pilot relay system," *Electrical Engineering*, vol. 57, no. 1, pp. 5–10, 1938.

[9] "How it all began," *OMICRON Magazine*, vol. 2, pp. 617–644, 2018.

[10] M. Benitez, J. Xavier, K. Smith, and D. Minshall, "Directional element design for protecting circuits with capacitive fault and load currents," in *Protective Relay Engineers (CPRE), 2018 71st Annual Conference for*. IEEE, 2018, pp. 1–11.

[11] J. J. Serna and J. M. López-Lezama, "An alternative method for obtaining the optimal directional characteristic angle of directional overcurrent relays in transmission networks," *Contemporary Engineering Sciences*, 2018.

[12] *SIPROTEC 5 Distance and Line Differential Protection Breaker Management for 1-Pole and 3-Pole Tripping 7SA87 7SD87 7SL87 7VK87*, Siemens A.G., July 2018.

[13] G. Ziegler, *Numerical distance protection: principles and applications*. John Wiley & Sons, 2011.

[14] H. Hermann, "digitale schutztechnik," *VDE-Verlag GmbH*, 1997.

[15] G. Li, B. Zhang, J. Wang, Z. Hao, Z. Bo, D. Writer, and T. Yip, "Wind farm electromagnetic dynamic model and outgoing line protection relay rtds testing," in *Universities' Power Engineering Conference (UPEC), Proceedings of 2011 46th International*. VDE, 2011, pp. 1–6.

[16] M. Walter, "Der selektivschutz nach dem widerstandsprinzip," Ph.D. dissertation, Techn. Hochschule Aachen., 1932.

[17] B. Hu, K. Xie, and H.-M. Tai, "Inverse problem of power system reliability evaluation: Analytical model and solution method," *IEEE Transactions on Power Systems*, 2018.

[18] S. Nikolovski, M. Havranek, and P. Marić, "Numerical relay protection coordination using simulation software," in *Information & Communication Technology Electronics & Microelectronics (MIPRO), 2013 36th International Convention on*. IEEE, 2013, pp. 869–873.

[19] C. international des grands réseaux électriques. Joint working group B5-214 (26), *Testing of Distance Protection Relays*. CIGRÉ, 2008.

[20] A. Sanchez-Ruiz, M. Mazuela, S. Alvarez, G. Abad, and I. Baraia, "Medium voltage–high power converter topologies comparison procedure, for a 6.6 kv drive application using 4.5 kv igbt modules," *IEEE Transactions on Industrial Electronics*, vol. 59, no. 3, pp. 1462–1476, 2012.

[21] E. Muljadi, N. Samaan, V. Gevorgian, J. Li, and S. Pasupulati, "Short circuit current contribution for different wind turbine generator types," in *Power and Energy Society General Meeting, 2010 IEEE*. IEEE, 2010, pp. 1–8.

[22] P. Pourbeik, "Wecc second generation wind turbine models," Electric Power Research Institute, Specification, January 2014.

[23] P. Sørensen, "International standard iec 61400-27-1:2015," International Electrotechnical Commission, Specification, February 2015.

[24] D. GmbH, "Template documentation dfig template," DIgSILENT, Template documentation, December 2017.

[25] C. international des grands réseaux électriques.Joint working group B5.37, *Protection, Monitoring and Control of Shunt Reactors*. CIGRÉ, 2013.

[26] F. T. Ulaby, E. Michielssen, and U. Ravaioli, "Fundamentals of applied electromagnetics 6e," *Boston, Massachussetts: Prentice Hall*, 2010.

[27] H. Nyquist, "Certain topics in telegraph transmission theory," *Transactions of the American Institute of Electrical Engineers*, vol. 47, no. 2, pp. 617–644, 1928.

[28] W. S. Meyer and T.-h. Liu, "Electromagnetic transient program theory book," *Portland, Oregon*, 1987.

[29] J. J. Grainger, W. D. Stevenson, W. D. Stevenson *et al.*, *Power system analysis*. Mcgraw-Hill Education - Europe, 2003, paragraph 9.9.

[30] L. He and C.-C. Liu, "Impact of lvrt capability of wind turbines on distance protection of ac grids," in *Innovative Smart Grid Technologies (ISGT), 2013 IEEE PES*. IEEE, 2013, pp. 1–6.

Appendices

Appendix 1

Scenario List

The following list gives all scenarios which are tested.

FileID	Fault Resistance (Ω)	Fault Location	Grid	Generated power (%)	Involved Lines
50033	0	1	Min	0	LG
50034	0	1	Max	0	LG
50035	0	1	Min	10	LG
50036	0	1	Max	10	LG
50037	0	1	Min	70	LG
50038	0	1	Max	70	LG
50041	2.25	1	Min	0	LG
50042	2.25	1	Max	0	LG
50043	2.25	1	Min	10	LG
50044	2.25	1	Max	10	LG
50045	2.25	1	Min	70	LG
50046	2.25	1	Max	70	LG
50057	0	1	Min	0	LLG
50058	0	1	Max	0	LLG
50059	0	1	Min	10	LLG
50060	0	1	Max	10	LLG
50061	0	1	Min	70	LLG
50062	0	1	Max	70	LLG
50065	2.25	1	Min	0	LLG
50066	2.25	1	Max	0	LLG
50067	2.25	1	Min	10	LLG
50068	2.25	1	Max	10	LLG
50069	2.25	1	Min	70	LLG
50070	2.25	1	Max	70	LLG
50113	2	1	Min	0	LLL
50114	2	1	Max	0	LLL
50115	2	1	Min	10	LLL
50116	2	1	Max	10	LLL
50117	2	1	Min	70	LLL
50118	2	1	Max	70	LLL
50153	0	2	Min	0	LG
50154	0	2	Max	0	LG
50155	0	2	Min	10	LG
50156	0	2	Max	10	LG
50157	0	2	Min	70	LG
50158	0	2	Max	70	LG
50159	0	2	Min	100	LG
50160	0	2	Max	100	LG
50161	1.2	2	Min	0	LG
50162	1.2	2	Max	0	LG
50163	1.2	2	Min	10	LG
50164	1.2	2	Max	10	LG
50165	1.2	2	Min	70	LG
50166	1.2	2	Max	70	LG
50167	1.2	2	Min	100	LG
50168	1.2	2	Max	100	LG
50177	0	2	Min	0	LLG
50178	0	2	Max	0	LLG
50179	0	2	Min	10	LLG

50180	0	2	Max	10	LLG
50181	0	2	Min	70	LLG
50182	0	2	Max	70	LLG
50183	0	2	Min	100	LLG
50184	0	2	Max	100	LLG
50185	1.7	2	Min	0	LLG
50186	1.7	2	Max	0	LLG
50187	1.7	2	Min	10	LLG
50188	1.7	2	Max	10	LLG
50189	1.7	2	Min	70	LLG
50190	1.7	2	Max	70	LLG
50191	1.7	2	Min	100	LLG
50192	1.7	2	Max	100	LLG
50201	0	2	Min	0	LL
50202	0	2	Max	0	LL
50203	0	2	Min	10	LL
50204	0	2	Max	10	LL
50205	0	2	Min	70	LL
50206	0	2	Max	70	LL
50207	0	2	Min	100	LL
50208	0	2	Max	100	LL
50209	1.7	2	Min	0	LL
50210	1.7	2	Max	0	LL
50211	1.7	2	Min	10	LL
50212	1.7	2	Max	10	LL
50213	1.7	2	Min	70	LL
50214	1.7	2	Max	70	LL
50215	1.7	2	Min	100	LL
50216	1.7	2	Max	100	LL
50225	0	2	Min	0	LLL
50226	0	2	Max	0	LLL
50227	0	2	Min	10	LLL
50228	0	2	Max	10	LLL
50229	0	2	Min	70	LLL
50230	0	2	Max	70	LLL
50231	0	2	Min	100	LLL
50232	0	2	Max	100	LLL
50233	1.7	2	Min	0	LLL
50234	1.7	2	Max	0	LLL
50235	1.7	2	Min	10	LLL
50236	1.7	2	Max	10	LLL
50237	1.7	2	Min	70	LLL
50238	1.7	2	Max	70	LLL
50239	1.7	2	Min	100	LLL
50240	1.7	2	Max	100	LLL
50273	0	3	Min	0	LG
50274	0	3	Max	0	LG
50275	0	3	Min	10	LG
50276	0	3	Max	10	LG
50277	0	3	Min	70	LG

50278	0	3	Max	70	LG
50279	0	3	Min	100	LG
50280	0	3	Max	100	LG
50281	0	3	Min	0	LLG
50282	0	3	Max	0	LLG
50283	0	3	Min	10	LLG
50284	0	3	Max	10	LLG
50285	0	3	Min	70	LLG
50286	0	3	Max	70	LLG
50287	0	3	Min	100	LLG
50288	0	3	Max	100	LLG
50289	0	3	Min	0	LL
50290	0	3	Max	0	LL
50291	0	3	Min	10	LL
50292	0	3	Max	10	LL
50293	0	3	Min	70	LL
50294	0	3	Max	70	LL
50295	0	3	Min	100	LL
50296	0	3	Max	100	LL
50297	0	3	Min	0	LLL
50298	0	3	Max	0	LLL
50299	0	3	Min	10	LLL
50300	0	3	Max	10	LLL
50301	0	3	Min	70	LLL
50302	0	3	Max	70	LLL
50303	0	3	Min	100	LLL
50304	0	3	Max	100	LLL
50329	0	4	Min	0	LG
50330	0	4	Max	0	LG
50331	0	4	Min	10	LG
50332	0	4	Max	10	LG
50333	0	4	Min	70	LG
50334	0	4	Max	70	LG
50335	0	4	Min	100	LG
50336	0	4	Max	100	LG
50337	0	4	Min	0	LLG
50338	0	4	Max	0	LLG
50339	0	4	Min	10	LLG
50340	0	4	Max	10	LLG
50341	0	4	Min	70	LLG
50342	0	4	Max	70	LLG
50343	0	4	Min	100	LLG
50344	0	4	Max	100	LLG
50345	0	4	Min	0	LL
50346	0	4	Max	0	LL
50347	0	4	Min	10	LL
50348	0	4	Max	10	LL
50349	0	4	Min	70	LL
50350	0	4	Max	70	LL
50351	0	4	Min	100	LL

50352	0	4	Max	100	LL
50353	0	4	Min	0	LLL
50354	0	4	Max	0	LLL
50355	0	4	Min	10	LLL
50356	0	4	Max	10	LLL
50357	0	4	Min	70	LLL
50358	0	4	Max	70	LLL
50359	0	4	Min	100	LLL
50360	0	4	Max	100	LLL
50385	0	5	Min	0	LG
50386	0	5	Max	0	LG
50387	0	5	Min	10	LG
50388	0	5	Max	10	LG
50389	0	5	Min	70	LG
50390	0	5	Max	70	LG
50394	0	5	Max	0	LLG
50395	0	5	Min	10	LLG
50396	0	5	Max	10	LLG
50397	0	5	Min	70	LLG
50401	0	5	Min	0	LL
50402	0	5	Max	0	LL
50403	0	5	Min	10	LL
50404	0	5	Max	10	LL
50405	0	5	Min	70	LL
50406	0	5	Max	70	LL
50409	0	5	Min	0	LLL
50410	0	5	Max	0	LLL
50411	0	5	Min	10	LLL
50412	0	5	Max	10	LLL
50413	0	5	Min	70	LLL
50414	0	5	Max	70	LLL

Appendix 2: Positive Sequence Circuit Decompositon

The scenario of unexpected result 5 is verified with a calculation. It is tried to clarify the situation and find a reason for the unexpected behavior.

In this scenario a three-phase fault is initiated at the 220 kV terminals of transformer Trf 1. This fault has a resistance of 1.7 Ω. The wind turbines are generating power at a nominal level. The external grid is set to its minimum grid strength.

The grid is assumed to be balanced and the fault is a balanced 3-phase fault. Therefore, the grid can be simplified to a positive sequence circuit. The fault location and the two protection relays all are located in the 220 kV area. All impedances and sources are converted to an equivalent as they are seen from the 220 kV area. With this method transformers are simplified to an impedance. The total equivalent circuit does only consist of resistance, reactance, and voltage source elements. The equivalent circuit can be found in figure A2-1. This circuit includes the fault.

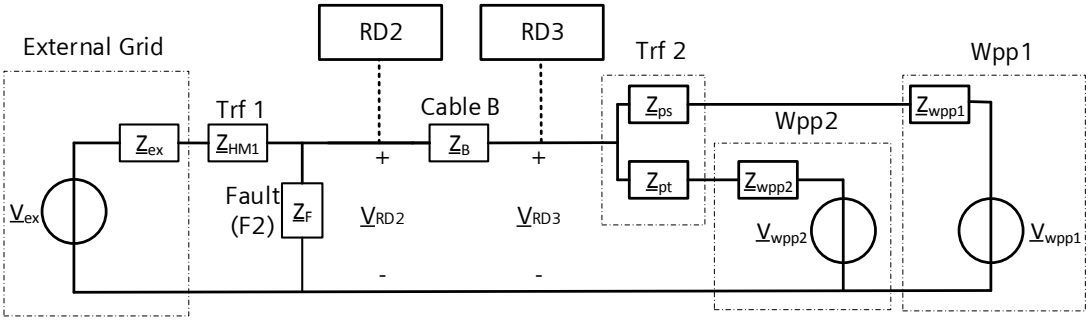

Figure A2-1: Equivalent positive sequence circuit including a thee phase fault at location F2.

Impedance calculation

The parameters needed for this calculation are listed in table A2-1. These values all are positive sequence values in the complex domain.

Table A2-1: Input parameters to calculate the positive sequence circuit.

Symbol	Description	Value
V_{eq}	Equivalent nominal voltage level	220 kV
C_{max}	Fault voltage factor	1.08
$\underline{Z}_{ex}$	Series impedance of the external grid	1.45+20.33 j Ω
$\underline{z}_{HM1}$	Per unit impedance of transformer 1 between the 380 kV to the 220 kV side	$(1.40+145j)*10^{-3}$ p.u.
S_{220-t1}	Rated power for the 220 kV side of transformer 1.	400 MVA
R_{t1}	Ratio of transformer 1	380/225
Z_{Fault}	Fault impedance	1.7 Ω
$\underline{Z}_B$	Total impedance of cable B	1.62 + 6.91 j Ω
$\underline{z}_{ps}$	Per unit impedance of transformer 1 between the 220 kV to the 66 kV side	$2.47\cdot10^{-3}+0.11j$ p.u.
S_{66-t1}	Rated power for the 66 kV side of transformer 2	226 MVA
$\underline{z}_{WTT}$	Per unit impedance of the wind turbine transformer	$(7.6+92.7j)10^{-3}$ Ω
S_{WTT}	Rated power for the wind turbine transformer.	8.8 MVA
V_{WPP}	Rated voltage of wind power plant	66 kV
$\underline{Z}_{WT}$	Impedance per wind turbine	$(1.2+11.7j)\cdot10^{-3}$ Ω
$\underline{Z}_{CWT}$	Impedance of the cable which connects the wind turbine string to the 66 kV bus	0.545+0.939j Ω

External grid

The voltage source voltage is given by:

$$V_{ex} = \frac{V_{eq}\cdot C_{Max}}{\sqrt{3}} \approx 137\ kV \tag{A2-1}$$

The external grid impedance Z_{ex} seen from the 220 side has to be converted using the transformer ratio:

$$\underline{Z}_{ex220} = \frac{\underline{Z}_{ex}}{R_{t1}^2} \approx 0.51+7.13j\ \Omega \tag{A2-2}$$

Transformer 1

Transformer 1 is a three-winding autotransformer. The tertiary winding is connected to a reactive power compensation bus. The amount of current flowing in this direction is neglectable. Therefore, only the primary en secondary side is considered. The impedance between the primary and secondary side is:

$$\underline{Z}_{HM1} = \underline{z}_{HM1}\cdot\frac{V_{eq}^2}{S_{220-t1}} \approx 0.17+17.55j\ \Omega \tag{A2-3}$$

Fault

The fault has in the positive sequence domain a resistance of 1.7 Ω

Transformer 2

Transformer 2 is a three-winding transformer. The primary winding is connected to the 220 kV side. The secondary and tertiary windings are connected to a wind power plant.

The impedance between the primary to secondary side ($\underline{Z}_{ps}$) and between the primary an tertiary side are equal (Z_{pt}).

$$\underline{Z}_{ps} = \underline{Z}_{pt} = \underline{z}_{ps} \cdot \frac{V_{eq}^2}{S_{66-t1}} \approx 0.58 + 28.10j\ \Omega \tag{A2-4}$$

Wind power plant

The wind power plants consist of three strings with each 8 wind turbines in parallel. Wind power plant 2 has 2 strings with 8 wind turbines and one string with 7 wind turbines in parallel. The equivalent impedance for one string is:

$$\underline{Z}_{wtS-n} = (\underline{Z}_{WT} + \underline{z}_{WTT}\frac{\underline{V}_{wt}^2}{\underline{S}_{WTT}})/n + \underline{Z}_{CWT} \tag{A2-5}$$

Where $\underline{V}_{wt}$ is the nominal voltage level of the wind power plant which is 66 kV and n is the number of wind turbines in the string. $\underline{Z}_{wtS-8} = 2.38 + 20.0j$ is the impedance for a string with 8 wind turbines. $\underline{Z}_{wtS-7} = 2.55 + 21.9j$ is the impedance for a string with 7 wind turbine. The equivalent impedance of wind power plant 1 seen from the 220 kV side is:

$$\underline{Z}_{WPP1} = \frac{\underline{Z}_{wtS-8}}{3} \cdot \frac{\underline{V}_{eq}^2}{\underline{V}_{wt}^2} \approx 9.65 + 81.0j\ \Omega \tag{A2-6}$$

The equivalent impedance of wind power plant 2 seen from the 220 kV side is:

$$\underline{Z}_{WPP2} = \frac{1}{\frac{2}{\underline{Z}_{wtS-8}} + \frac{1}{\underline{Z}_{wtS-7}}} \cdot \frac{\underline{V}_{eq}^2}{\underline{V}_{wt}^2} \approx 9.82 + 84.1j\ \Omega \tag{A2-7}$$

Simplification

The transformer 'trf 2' impedance and the two wind power plant impedances are merged. The simplified circuit can be found in figure A2-2. It is assumed that V_{Wpp1} and V_{Wpp2} are equal. The combined impedance is:

$$\underline{Z}_{WpTf} = 1/(\frac{1}{\underline{Z}_{wpp1} + \underline{Z}_{ps}} + \frac{1}{\underline{Z}_{wpp2} + \underline{Z}_{pt}}) \approx 5.12 + 56.7j\ \Omega \tag{A2-8}$$

Normal condition

In the normal condition $\underline{Z}_F$ is not present. A current of 1 A flows from the wind turbines to the external grid. The nominal voltage is at the connection point of the external grid. The only parallel impedance considered in the following calculation is the conductance and capacitance of cable B. Figure A2-2 shows the positive sequence circuit of the normal condition.

$\underline{V}_n$= $\frac{220}{\sqrt{3}}$ kV $\underline{/0^\circ}$

$\underline{I}_n$= 1 $\underline{/0^\circ}$ kA

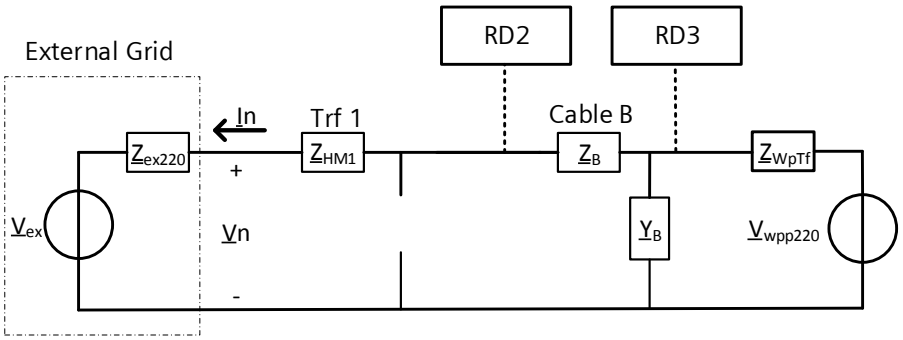

Figure A2-2: Equivalent positive sequence circuit where the WPP and transformer 2 are merged in normal condition.

RD2

The current in at RD2 is equal to the nominal current ($\underline{I}_{RD2} = \underline{I}_n$). The L-G voltage at RD2 is:

$$\underline{V}_{RD2} = \underline{V}_n + \underline{Z}_{HM1} * \underline{I}_n = 128\text{kV}\underline{/8^\circ} \tag{A2-9}$$

Cable B

Cable B is modeled with a distributed parameter model. The voltage and current on the receiving side of the cable is given by:

$$\begin{bmatrix} \underline{V}_{RD3} \\ \underline{I}_{RD3} \end{bmatrix} = A \begin{bmatrix} \underline{V}_{RD2} \\ \underline{I}_{RD2} \end{bmatrix} = \begin{bmatrix} cosh(\underline{\gamma} \cdot l) & -\underline{Z}_C \cdot sinh(\underline{\gamma} \cdot l) \\ \frac{1}{\underline{Z}_C} \cdot sinh(\underline{\gamma} \cdot l) & -cosh(\underline{\gamma} \cdot l) \end{bmatrix} \begin{bmatrix} \underline{V}_{RD2} \\ \underline{I}_{RD2} \end{bmatrix} \tag{A2-10}$$

Where:

$\underline{\gamma} =$	$\sqrt{\underline{Z'} \cdot \underline{Y'}}$	Propagation factor
$\underline{Z}_C =$	$\sqrt{\frac{\underline{Z'}}{\underline{Y'}}}$	Characteristic impedance
$\underline{Z'}$:		Series impedance per unit length
$\underline{Y'}$:		Parallel conductance per unit length

The Matrix A for cable B is given by:

$$A = \begin{bmatrix} 1.0015 - 0.0006j & 1.6222 + 6.9113j \\ (0.0012 + 1.9931j) \cdot 10^{-3} & 1.0047 - 0.0012j \end{bmatrix}$$

Equation A2-10 evaluated gives a voltage and current of:

$\underline{V}_{RD3} = 131.3 + 24.4j = 131\text{kV}\underline{/11^\circ}$
$\underline{I}_{RD3} = 0.969 + 0.252j = 1.002\text{kA}\underline{/14.5^\circ}$

Voltage angle wind turbine

The equivalent voltage of the V_{WPP} can now be approximated with:

$$\underline{V}_{WPP} = \underline{V}_{RD3} + \underline{I}_{RD3} \cdot \underline{Z}_{WPTf} = 144\text{kV}\underline{/34^\circ} \tag{A2-11}$$

Fault condition

Figure A2-3 shows the positive sequence circuit in fault condition.

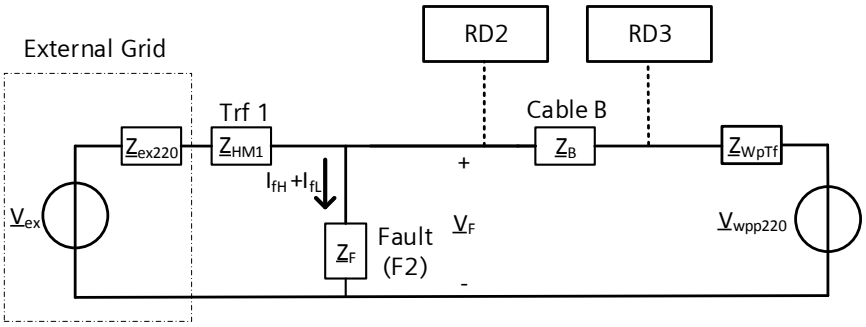

Figure A2-3: Equivalent positive sequence circuit where the WPP and transformer 2 are merged.

All the impedances are known now. The circuit is simplified. The next goal is to find the voltage and current of the protection relay locations in case of a fault.

Source voltage

During the fault the voltages $\underline{V}_{wpp220}$ and $\underline{V}_{ex}$ are equal to the normal condition

$$\underline{V}_{wpp220} = 144\text{kV}\angle 34^\circ \tag{A2-12}$$

Fault current

The impedance from the fault to the grid side can be combined into:

$$\underline{Z_H} = \underline{Z}_{ex220} + \underline{Z}_{HM1} \tag{A2-13}$$

The impedance from the WT side can be combined into:

$$\underline{Z_L} = \underline{Z}_B + \underline{Z}_{WpTf} \tag{A2-14}$$

The fault current contribution from the grid side is:

$$\underline{I}_{fH} = \frac{V_{ex} \cdot \underline{Z_H}}{\underline{Z_L} \cdot \underline{Z_H} + \underline{Z_F} + \underline{Z_L} + \underline{Z_L} \cdot \underline{Z_F}} \approx -0.65 + 4.9j\ kA \tag{A2-15}$$

The fault current contribution from the WPP side is:

$$\underline{I}_{fH} = \frac{\underline{V}_{wpp220} \cdot \underline{Z_L}}{\underline{Z_H} \cdot \underline{Z_L} + \underline{Z_H} + \underline{Z_H} + \underline{Z_H} \cdot \underline{Z_F}} \approx -1.51 + 1.65j\ \Omega \tag{A2-16}$$

The total fault current is

$$\underline{I}_f = \underline{I}_{fL} + \underline{I}_{fH} = -2.16 + 6.56j\ kA \tag{A2-17}$$

Measurement points RD2 and RD3

The current at RD2 and RD3 is:

$$\underline{I}_{RD2} = \underline{I}_{RD3} = \frac{\underline{V}_{wpp220} - \underline{V}_f}{\underline{Z}_H} \approx 1.62 - 1.65j; \tag{A2-18}$$

The voltage at RD2 in polar form is:

$$\underline{V}_{RD2} = \underline{V}_F = \underline{I}_{fL} \cdot \underline{Z}_F \approx 11.7\text{kV}\underline{/-72^\circ} \tag{A2-19}$$

The voltage at RD3 in polar form is:

$$\underline{V}_{RD3} = \underline{I}_{RD3} \cdot \underline{Z}_L \approx 17.9\text{kV}\underline{/-9^\circ} \tag{A2-20}$$

The impedance at RD2 in polar form is:

$$\underline{Z}_{RD2} = \frac{\underline{V}_{RD2}}{\underline{I}_{RD2}} \approx 5\underline{/-26^\circ}\Omega \tag{A2-21}$$

The relay is measuring towards the WPP. therefore, the impedance is inverted with a minus sign.

$$\underline{Z}_{RD3} = -\frac{\underline{V}_{RD3}}{\underline{I}_{RD3}} \approx 7.6\underline{/-143^\circ}\Omega \tag{A2-22}$$

Comparison normal operation and fault condition

The table below gives a comparison between the normal condition and fault condition.

	Normal operation	Fault condition	Difference
$\angle V_{WPP}$	34°	34°	34°
$\angle V_{RD2}$	8°	-72°	80°
$\angle V_{RD3}$	11°	-9°	20°

Appendix 3: Sequential sequence Circuit decompositon

The scenario of unexpected result 6 is verified with a calculation. It is tried to clarify the situation and find a reason for the unexpected behavior.

In this scenario a two-phase to ground fault is initiated at the 380 kV terminals of transformer Trf 1. This fault has a resistance of 2.25 Ω. The wind turbines are generating power at 10% of nominal level. The external grid is set to its minimum grid strength.

The grid is assumed to be unbalanced and the fault is a two-phase to ground. The grid can be converted to a sequential components circuit consisting of a positive sequence, negative sequence and zero-sequence circuit. The considered protection relay RD3 is located in the 220 kV area. All impedances, sources and the fault are converted to an equivalent as they are seen from the 220 kV area. With this method transformers are simplified to an impedance. The total equivalent circuit does only consist of resistance, reactance, and voltage source elements. The equivalent circuit can be found in figure A3-1. This circuit includes the fault circuit denoted with a blue color.

The impedance values of the positive-sequence circuit and negative-sequence circuit are equal. The method of determining these values can be found in appendix 2.

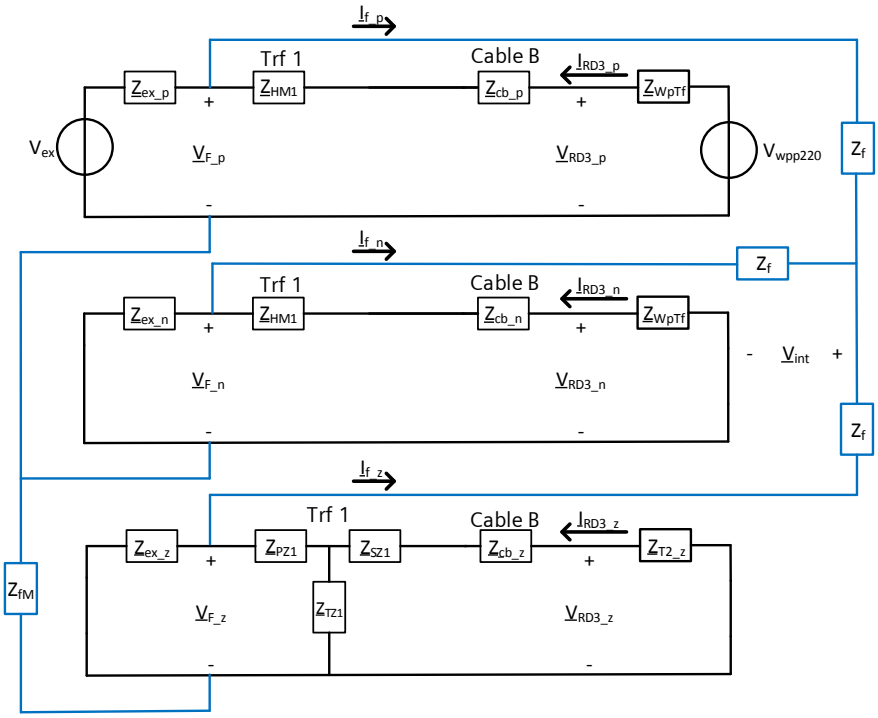

Figure A3-1: Equivalent sequential sequence circuit including a thee-phase fault at location F2.

Positive and negative sequence impedances

The impedances and voltages for the sequential sequence circuit are listed in A3-1. These values all are in the complex domain.

Table A3-1: Positive and negative sequence impedances.

Symbol pos. seq.	Symbol neg. seq.	Description	Value
V_{ex}		Equivalent nominal voltage level of the external grid	137 kV
V_{wpp220}		Equivalent nominal voltage level of the wind turbines	137 kV
$\underline{Z}_{ex\_p}$	$\underline{Z}_{ex\_n}$	External grid impedance	$0.51 + 7.13j\ \Omega$
$\underline{Z}_{HM1}$	$\underline{Z}_{HM1}$	Transformer impedance from primary to secondary side	$0.170 + 17.6j\ \Omega$
$\underline{Z}_{CB_p}$	$\underline{Z}_{CB_Z}$	Impedance of cable B	$1.62 + 6.91j\ \Omega$
$\underline{Z}_{WpTf}$	$\underline{Z}_{WpTf}$	Combined impedance of the wind power plant including transformer trf 2	$5.01 + 123j\ \Omega$

Zero sequence impedances

Table A3-2 shows the parameters needed to calculate the impedance in the zero sequence circuit.

Table A3-2: Parameters to calculate the zero sequence impedances.

Symbol	Description	Value
$\underline{Z}_{ex380\_z}$	External grid impedance	$2.69+25.6j\ \Omega$
$\underline{z}_{PS1\_z}$	Per unit impedance of transformer 1 from the primary to secondary side	$1.41\cdot10^{-3}+0.141j$ p.u.
z_{ST1_z}	Per unit impedance of transformer 1 from the secondary to tertiary side	$1.70\cdot10^{-3}+0.060j$ p.u.
$\underline{z}_{TP1\_z}$	Per unit impedance of transformer 1 from the tertiary to primary side	$1.70\cdot10^{-3}+0.088j$ p.u.
S_{TP1}	Rated power at the primary side of transformer 1	400 MVA
S_{TZ1}	Rated power at the secondary side of transformer 1	72 MVA
V_{TP1}	Rated voltage primary side transformer 1	380 kV
V_{TS1}	Rated voltage secondary side transformer 1	225 kV
$\underline{Z}_{CB\_z}$	Impedance cable B	$17.4+9.98j\ \Omega$
$\underline{z}_{PS2\_z}$	Per unit impedance of transformer 2 from the primary to secondary side	$2.47\cdot10^{-3}+0.12j$ p.u.
$\underline{z}_{ST2\_z}$	Per unit impedance of transformer 2 from the secondary to tertiary side	$4.5\cdot10^{-3}+0.22j$ p.u.
$\underline{z}_{TP2\_z}$	Per unit impedance of transformer 2 from the tertiary to primary side	$2.47\cdot10^{-3}+0.12j$ p.u.
S_{TP2}	Rated power at the primary side of transformer 2	226 MVA
$\underline{V}_{TP2}$	Rated voltage primary side transformer 2	230 kV
$\underline{V}_{TS2}$	Rated voltage secondary side transformer 2	66 kV

External grid

The external grid impedance Z_{ex_z} seen from the 220 kV side has to be converted using the transformer ratio:

$$\underline{Z}_{ex\_z}=\underline{Z}_{ex380\_z}\cdot\frac{V_{TS1}^2}{V_{TP1}^2}\approx0.942+8.98j\ \Omega \tag{A3-1}$$

Transformer 1

The transformer impedances are given in per unit values. These are converted with the following equations to an equivalent impedance as seen from the 220 kv side:

$$\begin{aligned}\underline{Z}_{PS1\_Z}&=\underline{z}_{PS1\_z}\cdot\frac{V_{TS1}^2}{S_{TP1}}\approx0.18+17.8j\ \Omega\\ \underline{Z}_{ST1\_Z}&=\underline{z}_{ST1\_z}\cdot\frac{V_{TS1}^2}{S_{TS1}}\approx1.20+62.1j\ \Omega\\ \underline{Z}_{TP1\_Z}&=\underline{z}_{TP1\_z}\cdot\frac{V_{TS1}^2}{S_{TS1}}\approx1.20+42.5j\ \Omega\end{aligned} \tag{A3-2}$$

The shared star point of the primary and secondary side of transformer 1 are connected to ground. In the zero-sequence this is represented as impedances in a y-configuration. The following transformation is used to determine the zero-sequence impedances:

$$\begin{aligned}\underline{Z}_{PZ1}&=(\underline{Z}_{PS1\_Z}-\underline{Z}_{ST1\_Z}+\underline{Z}_{TP1\_Z})/2\approx0.0886+18.7j\Omega\\ \underline{Z}_{SZ1}&=(\underline{Z}_{PS1\_Z}+\underline{Z}_{ST1\_Z}-\underline{Z}_{TP1\_Z})/2\approx0.0886-0.922j\Omega\\ \underline{Z}_{TZ1}&=(-\underline{Z}_{PS1\_Z}+\underline{Z}_{ST1\_Z}+\underline{Z}_{TP1\_Z})/2\approx1.11+43.4j\Omega\end{aligned} \tag{A3-3}$$

Transformer 2

The transformer impedances are given in per unit values. These are converted with the following equations to an equivalent impedance as seen from the 220 kv side:

$$\begin{aligned}\underline{Z}_{PS2\_Z} &= \underline{z}_{PS2\_z} \cdot \frac{V_{TS2}^2}{S_{TP2}} \approx 0.178 + 17.8\,j\Omega \\ \underline{Z}_{ST2\_Z} &= \underline{z}_{ST2\_z} \cdot \frac{V_{TS2}^2}{S_{TP2}} \approx 1.20 + 62.1\,j\Omega \\ \underline{Z}_{TP2\_Z} &= \underline{z}_{TP2\_z} \cdot \frac{V_{TS2}^2}{S_{TP2}} \approx 1.20 + 42.5\,j\Omega\end{aligned} \tag{A3-4}$$

Transformer 2 is a three-winding transformer. The primary winding is connected to the 220 kV side. The secondary and tertiary windings are connected to a wind power plant. The primary side of the transformer is in y-configuration with a grounded star point. The following transformation is used to determine the zero sequence impedances:

$$\begin{aligned}\underline{Z}_{PZ2} &= (\underline{Z}_{PS2\_Z} - \underline{Z}_{ST2\_Z} + \underline{Z}_{TP2\_Z})/2 \approx 0.0886 + 18.7\,j\Omega \\ \underline{Z}_{SZ2} &= (\underline{Z}_{PS2\_Z} + \underline{Z}_{ST2\_Z} - \underline{Z}_{TP2\_Z})/2 \approx 0.0886 - 0.922\,j\Omega \\ \underline{Z}_{TZ2} &= (-\underline{Z}_{PS2\_Z} + \underline{Z}_{ST2\_Z} + \underline{Z}_{TP2\_Z})/2 \approx 1.11 + 43.4\,j\Omega\end{aligned} \tag{A3-5}$$

The zero sequence current will flow through this ground connection. None of the zero-sequence current will flow to the wind power plant.

$$\underline{Z}_{T2\_Z} = \underline{Z}_{PZ2} + (\underline{Z}_{SZ2} || \underline{Z}_{TZ2}) \tag{A3-6}$$

Where the || operator calculates the parallel impedance.

Fault impedance

Two types of fault impedances are modeled. An independent ($\underline{Z}_f$) and a mutual ($\underline{Z}_m$) fault impedance. Figure A3-2 shows how these fault impedances appear in a three-phase system.

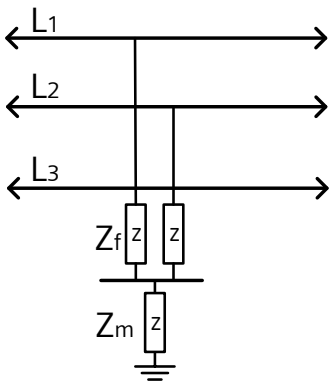

Figure A3-2: Impedances in a L-L-G fault in a three phase system

The $\underline{Z}_f$ fault in the sequence components circuit is split into three parts. In the considered scenario Z_{f380} has a value of 2.25 Ω and $\underline{Z}_m$ is zero. The values appear lower at the 220 kV side. $\underline{Z}_{f380}$ at the 220 kV side is:

$$\underline{Z}_f = \underline{Z}_{f380} \cdot \frac{V_{TS1}^2}{V_{TP1}^2} = 0.789\Omega \tag{A3-7}$$

Fault condition

All the impedances are known now. The next goal is to find the voltage and current of the protection relay locations in case of a fault.

Equivalent impedances

The following equivalent impedances are defined:

$$\begin{aligned}
&\underline{Z}_{L_P} = \underline{Z}_{L_N} = \underline{Z}_{HM1} + \underline{Z}_{CB_P} + \underline{Z}_{WpTf} \\
&\underline{Z}_{L_Z} = ((\underline{Z}_{T2_Z} + \underline{Z}_{CB_Z} + \underline{Z}_{SZ1}) || \underline{Z}_{TZ1}) + \underline{Z}_{PZ1} + \underline{Z}_{fm} \\
&\underline{Z}_{fp} = (\underline{Z}_{L_P} || \underline{Z}_{ex_p}) + \underline{Z}_f + (((\underline{Z}_{L_N} || \underline{Z}_{ex_N}) + \underline{Z}_f) || ((\underline{Z}_{L_Z} || \underline{Z}_{ex_Z}) + \underline{Z}_f)
\end{aligned} \tag{A3-8}$$

Fault current and fault voltage

The positive sequence fault current can be calculated with:

$$\underline{I}_{f\_p} = \frac{\underline{V}_{ex\_p}}{\underline{Z}_{fp}} \tag{A3-9}$$

The positive-sequence fault voltage is given by:

$$\underline{V}_{f\_p} = V_{ex} - \underline{I}_{f\_p} \cdot (\underline{Z}_{L\_P} || \underline{Z}_{ex\_p}) \tag{A3-10}$$

The internal voltage of the node between the three spitted fault resistances is:

$$\underline{V}_{fint} = \underline{V}_{f\_p} - \underline{I}_{f\_p} \cdot \underline{Z}_f \tag{A3-11}$$

The negative and zero sequence fault current and voltage can be calculated using:

$$\begin{aligned}
\underline{I}_{f_N} &= \frac{\underline{V}_{fint}}{\underline{Z}_{ex_n} || \underline{Z}_{L_N} + \underline{Z}_f} \\
\underline{V}_{f_N} &= \underline{V}_{fint} - \underline{I}_{f_N} \cdot \underline{Z}_f \\
\underline{I}_{f_z} &= \frac{\underline{V}_{fint}}{\underline{Z}_{ex_z} || \underline{Z}_{L_z} + \underline{Z}_f + \underline{Z}_{fm}} \\
\underline{V}_{f_z} &= \underline{V}_{fint} - \underline{I}_{f_z} (\underline{Z}_f + \underline{Z}_{fm})
\end{aligned} \tag{A3-12}$$

Current and voltage at RD3

The voltage and currents at RD3 can be calculated using:

$$
\begin{aligned}
\underline{I}_{RD3\_P} &= \frac{\underline{V}_{wpp220} - \underline{V}_{f\_p}}{\underline{Z}_{L\_P}} \\
\underline{V}_{RD3\_P} &= \underline{V}_{wpp220} - \underline{I}_{RD3\_P} \cdot \underline{Z}_{WpTf} \\
\underline{I}_{RD3\_N} &= \frac{\underline{V}_{f\_N}}{\underline{Z}_{L\_N}} \\
\underline{V}_{RD3\_N} &= \underline{I}_{RD3\_N} \cdot \underline{Z}_{WpTf} \\
\underline{I}_{RD3\_Z} &= \underline{V}_{f\_z} \cdot \frac{\underline{Z}_{L\_Z} - \underline{Z}_{TP1\_Z}}{\underline{Z}_{L\_Z} \cdot (\underline{Z}_{TS1\_Z} + \underline{Z}_{CB\_Z} + \underline{Z}_{T2\_z})} \\
\underline{V}_{RD3\_Z} &= \underline{I}_{RD3\_Z} \cdot \underline{Z}_{T2\_z}
\end{aligned}
\tag{A3-13}
$$

Transformation to ABC basis

A matrix vector transformation can transform the values from a DQ0 basis to a ABC basis. The transformation which is used is:

$$\overrightarrow{V_{abc}} = A \cdot \overrightarrow{V_{dqz}} \tag{A3-14}$$

Where

1. A is the transformation matrix $\begin{bmatrix} 1 & 1 & 1 \\ 1 & \underline{a}^2 & \underline{a} \\ 1 & \underline{a} & \underline{a}^2 \end{bmatrix}$.
2. $\underline{a}= -0.5 + \frac{\sqrt{3} \cdot j}{2}$
3. $\overrightarrow{V_{dqz}}$ is the sequential components vector $\overrightarrow{V_{dqz}} = \begin{bmatrix} \underline{V}_p \\ \underline{V}_n \\ \underline{V}_z \end{bmatrix}$
4. $\overrightarrow{V_{abc}}$ is the vector with values for each line $\begin{bmatrix} \underline{V}_a \\ \underline{V}_b \\ \underline{V}_c \end{bmatrix}$

This transformation can be used to transform voltages as well as currents and impedances.

The voltage phasors at the fault location and the he voltage and current phasors location of RD3 can be found in table A3-3.

Table A3-3: Line voltages and currents at fault location and at RD3

Symbol	Line a	Line b	Line c	Description
$\underline{V}_f$	15 kV $\angle 162°$	15 kV $\angle 40°$	139 kV $\angle -1°$	L-G voltages at fault location
$\underline{V}_{RD3}$	53 kV $\angle -165°$	42 kV $\angle 133°$	112 kV $\angle 0°$	L-G voltages at RD3
$\underline{I}_{RD3}$	1.40 kA $\angle 149°$	1.03 kA $\angle 70°$	0.53 kA $\angle 130°$	Line impedances at RD3

Impedance calculation

The protection relay RD3 calulates the impedance from $\overrightarrow{V_{RD3}}$ and $\overrightarrow{I_{RD3}}$. The ground current is calculated with:

$$\underline{I}_G = -\underline{I}_a - \underline{I}_b - \underline{I}_c \tag{A3-15}$$

The $L-G$ resistance and reactance can be calculated with the following equation using phasors:

$$R_{L-G} = \frac{|U_{L-G}|}{|I_L|} \cdot \frac{cos(\varphi_U - \varphi_{I_L}) - \frac{|I_G|}{|I_L|} \dot{k}_X \cdot cos(\varphi_U - \varphi_{I_G})}{1 - (k_X + k_R) \cdot \frac{|I_G|}{|I_L|} \cdot cos(\varphi_{I_G} - \varphi_{I_L}) + k_R \cdot k_X \cdot (\frac{|I_G|}{|I_L|})^2} \tag{A3-16}$$

$$X_{L-G} = \frac{|U_{L-G}|}{|I_L|} \cdot \frac{sin(\varphi_U - \varphi_{I_L}) - \frac{|I_G|}{|I_L|} \cdot k_R \cdot sin(\varphi_U - \varphi_{I_G})}{1 - (k_X + k_R) \cdot \frac{|I_G|}{|I_L|} \cdot cos(\varphi_{I_G} - \varphi_{I_L}) + k_R \cdot k_X \cdot (\frac{|I_G|}{|I_L|})^2} \tag{A3-17}$$

Where:

$\|U_{L-G}\|$:	Magnitude of line to ground voltage component
φ_U:	Angle of the phase to ground voltage
$\|I_L\|$:	Magnitude of the phase current component
φ_{I_L}:	Angle of the phase current
$\|I_G\|$:	Magnitude of the earth current component
φ_{I_G}:	Angle of the ground current
k_R:	Real part of the residual compensation factor in RD3 defined as 3.25
k_X:	Imaginary part of the residual compensation factor in RD3 defined as 0.15.

Equation A3-16 and A3-17 evaluated gives the following impedances:

$\underline{Z}_{L1-G}$=3.83+30.9j Ω
$\underline{Z}_{L2-G}$=3.67+12.3j Ω
$\underline{Z}_{L3-G}$=-7.80+110.0j Ω

Appendix 4: Determination of the real loop impedance of unexpected result 6

The scenario of unexpected result 6 is verified with a calculation. It is tried to clarify the situation and find a reason for the unexpected behavior. It is found that the calculated fault loop impedance is different from the real fault loop impedance. In this appendix is given what the real fault loop impedance should be if all information was available for the calculation.

L-G fault loop

Figure A4-1 gives the fault loop of Line b to ground. The thin dashed line gives the influencing circuits.

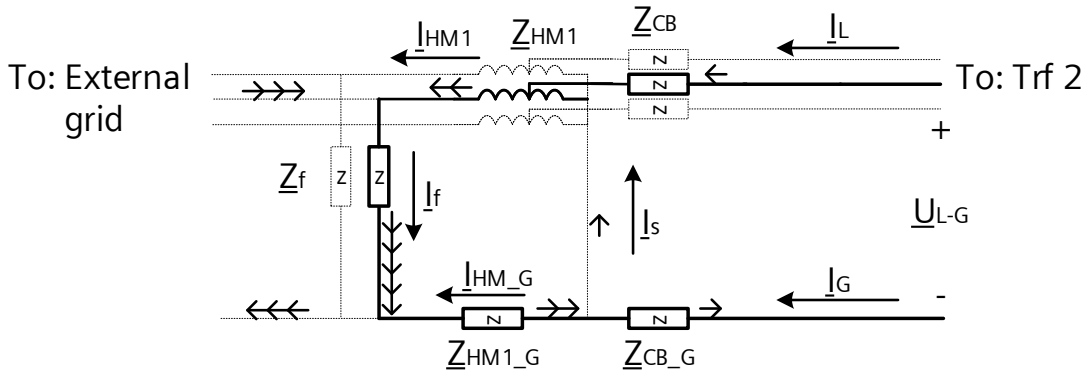

Figure A4-1: $L_B - G$ fault loop with influencing circuit in dashed line.

The involved impedances, voltages and currents are determined in appendix 2 and 3. These values are listed in table A4-1.

Table A4-1: Voltages, currents and impedances in the fault loop that effect the fault loop impedance.

Symbol	Description	Value
$\underline{U}_{L_B-G}$	L-G voltage measured by the protection relay at line B	53 kV $\angle -165°$
$\underline{I}_{L_B}$	Line current measured by the protection relay through line B	$1.4kA\angle 148°$
$\underline{I}_G$	Ground current calculated by the protection relay	2.4 kA $\angle -61°$
$\underline{I}_{T1_B}$	Equivalent line current through line B of transformer 1 at the primary side	1.4 kA $\angle 148°$
$\underline{I}_{T1\_G}$	Equivalent ground current of transformer 1 at the primary side	2.4 kA $\angle -61°$
$\underline{Z}_{CB}$	Total line impedance of cable B	$1.62+6.91j\ \Omega$
$\underline{Z}_{CB\_G}$	Total ground impedance of cable B	$17.4+9.98j\ \Omega$
$\underline{Z}_{HM1}$	Equivalent line impedance of transformer 1 from the primary to secondary side	$0.177+18.3j\ \Omega$
$\underline{Z}_{HM\_G}$	Equivalent ground impedance of transformer 1 from the primary to secondary side	$0.177+17.8j\ \Omega$
$\underline{I}_{ex_B}$	Fault current contribution of the external grid	18.1 kA $\angle 164°$

Fault loop

Kirchhoff's voltage law for the L-G loop gives the following equation:

$$\underline{U}_{L-G} = \underline{I}_L * \underline{Z}_{CB} + \underline{I}_{T1} * \underline{Z}_{HM1} + (\underline{I}_{T1} + \underline{I}_{EX}) * \underline{Z}_f - \underline{I}_{T1\_G} * \underline{Z}_{HM1\_G} - \underline{I}_G * \underline{Z}_{CB\_G} \quad \text{(A4-1)}$$

The current through the transformer can be spit using the current through the star point (I_s).

$$\underline{I}_s = \underline{I}_{HM1} - \underline{I}_L = \frac{\underline{I}_{HM\_G} - \underline{I}_{L\_G}}{3} \quad \text{(A4-2)}$$

Equation A4-1 combined with A4-2 gives:

$$\overbrace{\underline{U}_{L-G} = \underline{I}_L * (\underline{Z}_{CB} + \underline{Z}_{HM1}) - \underline{I}_G * (\underline{Z}_{HM\_G} + \underline{Z}_{CB\_G})}^{\text{Loop voltage assumed by the protection relay}} + \overbrace{\underline{I}_s * (\underline{Z}_{HM1} + 3 * \underline{Z}_{HM\_G})}^{\text{Voltage caused by the grounded star point}} + \overbrace{(\underline{I}_s + \underline{I}_L + \underline{I}_{ex}) * \underline{Z}_f}^{\text{Fault voltage}} \quad \text{(A4-3)}$$

The tree parts of the equation can be composed so that:

$$\overbrace{\underline{U}_{L-G} = \underline{U}_{nl}}^{\text{Loop voltage assumed by the protection relay}} + \overbrace{\underline{U}_s}^{\text{Voltage caused by the grounded star point}} + \overbrace{\underline{U}_f}^{\text{Fault voltage}} \quad \text{(A4-4)}$$

Alternative residual compensation factor

The alternative residual compensation factor for this fault loop is:

$$\underline{k}_{alt} = k_{r\_alt} + k_{x\_alt} \cdot j = \frac{real(\underline{Z}_{HM\_G} + \underline{Z}_{CB\_G} - \underline{Z}_{HM1} - \underline{Z}_{CB})}{3 \cdot real(\underline{Z}_{HM1} + \underline{Z}_{CB})} + \frac{imag(\underline{Z}_{HM\_G} + \underline{Z}_{CB\_G} - \underline{Z}_{HM1} - \underline{Z}_{CB})}{3 \cdot imag(\underline{Z}_{HM1} + \underline{Z}_{CB})} j \quad \text{(A4-5)}$$

This evaluated gives $\underline{k}_{alt} = 2.92 + 0.03j$.
The k-factor combined with $\underline{U}_{nl}$

$$\underline{U}_{nl} = \underline{I}_L * (\underline{Z}_{CB} + \underline{Z}_{HM1}) - \underline{I}_{T1\_G} * (k_r * (\underline{R}_{HM} + \underline{R}_{CB}) + (j * k_x * (\underline{X}_{HM} + \underline{X}_{CB})) \quad \text{(A4-6)}$$

The $L_B - G$ impedance calculated by the protection relay with equations 2.4 and 2.4: $Z_{L_B-G} = -3.6 - 16.9j$.

Star point current

The current I_s influences the calculated impedance. If this term is included in the impedance calculation equations 2.4 and 2.4 can be rewritten as:

$$R_{L-G} = \frac{(Real(\underline{U}_L - \underline{U}_s)) \cdot Real(\underline{I}_X) + (Imag(\underline{U}_L) - Imag(\underline{U}_s)) \cdot imag(\underline{I}_X)}{Real(\underline{I}_R) \cdot Real(\underline{I}_X) + Imag(\underline{I}_R) \cdot Imag(\underline{I}_X)} \quad \text{(A4-7)}$$

$$X_{L-G} = \frac{Imag(\underline{U}_L - \underline{U}_s) \cdot Real(\underline{I}_R) - (Real(\underline{U}_L) - Real(\underline{U}_s)) \cdot imag(\underline{I}_R)}{Real(\underline{I}_R) \cdot Real(\underline{I}_X) + Imag(\underline{I}_R) \cdot Imag(\underline{I}_X)} \quad \text{(A4-8)}$$

Where the voltage drop due to the star point current is given by $\underline{V}_s = \underline{I}_s * (\underline{Z}_{HM1} + 3 * \underline{Z}_{HM\_G})$. $\underline{I}_R$ and $\underline{I}_X$ are composed currents given by:

$$\underline{I}_R = \underline{I}_L - k_r \cdot \underline{I}_E$$
$$\underline{I}_X = \underline{I}_L - k_x \cdot \underline{I}_E$$

This evaluated gives an calculated impedance of: $\underline{Z}_{L_B-G} = 3.2 + 8.0j\ \Omega$

Fault voltage

The fault voltage can be compensated in the equations A4-7 and A4-8 in a similar way as the star point current.

$$R_{L-G} = \frac{Real(\underline{U}_L - \underline{U}_f) \cdot Real(\underline{I}_X) + Imag(\underline{U}_L - \underline{V}_s) \cdot imag(\underline{I}_X)}{Real(\underline{I}_R) \cdot Real(\underline{I}_X) + Imag(\underline{I}_R) \cdot Imag(\underline{I}_X)} \quad \text{(A4-9)}$$

$$X_{L-G} = \frac{Imag(\underline{U}_L - \underline{U}_f) \cdot Real(\underline{I}_R) - Real(\underline{U}_L - \underline{U}_s) \cdot imag(\underline{I}_R)}{Real(\underline{I}_R) \cdot Real(\underline{I}_X) + Imag(\underline{I}_R) \cdot Imag(\underline{I}_X)} \quad \text{(A4-10)}$$

This evaluated gives an calculated impedance of: $\underline{Z}_{L_B-G} = -2.1 - 25.3j\ \Omega$

Including all corrections

The real loop impedance can be calculated by combining the three previous corrections. The combined equation to calculate the loop impedance is:

$$R_{L-G} = \frac{Real(\underline{U}_L - \underline{U}_s - \underline{U}_f) \cdot Real(\underline{I}_X) + Imag(\underline{U}_L - \underline{U}_s - \underline{U}_f) \cdot imag(\underline{I}_X)}{Real(\underline{I}_R) \cdot Real(\underline{I}_X) + Imag(\underline{I}_R) \cdot Imag(\underline{I}_X)} \quad \text{(A4-11)}$$

$$X_{L-G} = \frac{Imag(\underline{U}_L - \underline{U}_s - \underline{U}_f) \cdot Real(\underline{I}_R) - Real(\underline{U}_L - \underline{U}_s - \underline{U}_f) \cdot imag(\underline{I}_R)}{Real(\underline{I}_R) \cdot Real(\underline{I}_X) + Imag(\underline{I}_R) \cdot Imag(\underline{I}_X)} \quad \text{(A4-12)}$$

$\underline{I}_R$ and $\underline{I}_X$ are composed currents given by:

$$\underline{I}_R = \underline{I}_L - k_{r\_alt} \cdot \underline{I}_E$$
$$\underline{I}_X = \underline{I}_L - k_{x\_alt} \cdot \underline{I}_E$$

This evaluated gives an calculated impedance of: $\underline{Z}_{L_B-G} = -1.7 - 24.0j\ \Omega$

L-L Fault loop

The thick line in figure A4-2 is the L-L fault loop.

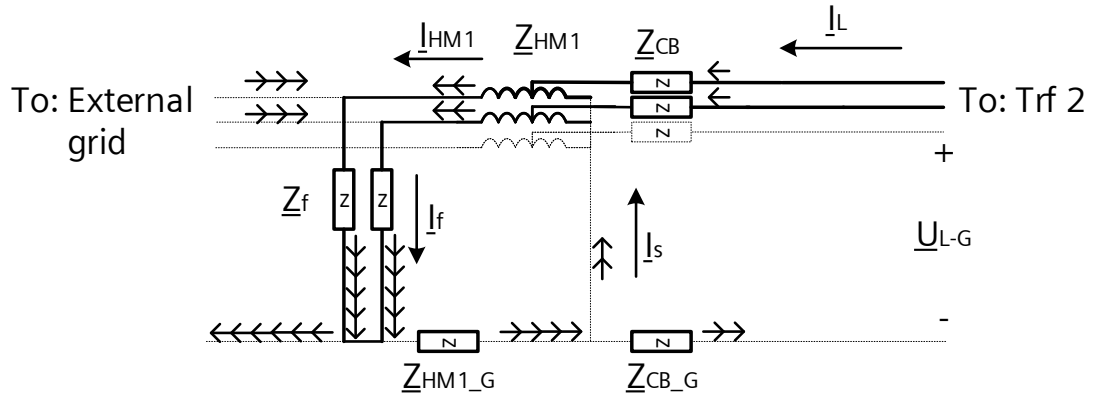

Figure A4-2: $L_A - L_B$ fault loop with influencing circuit in dashed line.

Kirchhoff's voltage law for the L-L loop gives the following equation:

$$\underline{U}_{L-L} = \underline{I}_{L_A} * \underline{Z}_{CB} + \underline{I}_{T1_A} * \underline{Z}_{HM1} + (\underline{I}_{T1_A} + \underline{I}_{EX_A}) * \underline{Z}_f - \underline{I}_{L_B} * \underline{Z}_{CB} - \underline{I}_{T1_B} * \underline{Z}_{HM1} - (\underline{I}_{T1_B} + \underline{I}_{EX_B}) * \underline{Z}_f \quad \text{(A4-13)}$$

Where:

$\underline{U}_{L-L} = \underline{U}_{L_A-G} - \underline{U}_{L_B-G}$
$\underline{I}_{T1_A} = \underline{I}_S + \underline{I}_{L_A}$
$\underline{I}_{T1_B} = \underline{I}_S + \underline{I}_{L_B}$

The L-L impedance is calculated by the protection relay with:

$$\underline{Z}_{L_A-L_B} = \frac{\underline{U}_{L_A-G} - \underline{U}_{L_B-G}}{\underline{I}_{L_A} - \underline{I}_{L_B}} \quad \text{(A4-14)}$$

Evaluated for the current scenario does this give an impedance of: $\underline{Z}_{L_A-L_B} = 18.6 + 25.67 * j$
The residual compensation factor is not applicable in this equations since the fault loop does not contain a ground impedance. The voltage induced by the star point current is canceled out. The fault voltage do lead to deviations in the impedance calculation.

Fault voltage

The fault voltages in the fault loop are:

$$\underline{U}_{f_A} = (\underline{I}_s + \underline{I}_{L_A} + \underline{I}_{ex_A}) * \underline{Z}_f \underline{U}_{f_B} = (\underline{I}_s + \underline{I}_{L_B} + \underline{I}_{ex_B}) * \underline{Z}_f \quad \text{(A4-15)}$$

The voltages are subtracted in equation A4-14. Therefore, the compensation voltage is:

$$\underline{U}_{f_{AB}} = \underline{U}_{f_A} - \underline{U}_{f_B} = (\underline{I}_{L_A} + \underline{I}_{ex_A} - \underline{I}_{L_B} - \underline{I}_{ex_B}) * \underline{Z}_f \quad \text{(A4-16)}$$

$\underline{U}_{f_{AB}}$ evaluated gives: -26.1-4.8 j Ω The compensated loop impedance equation is:

$$\underline{Z}_{L_A-L_B} = \frac{\underline{U}_{L_A-G} - \underline{U}_{L_B-G} - \underline{U}_{f_{AB}}}{\underline{I}_{L_A} - \underline{I}_{L_B}} \quad \text{(A4-17)}$$

This evaluated gives: 1.8+25.2 j Ω. This is equal to $\underline{Z}_{cb} + \underline{Z}_{HM1}$.